NASA
Technical
Paper
3116

September 1991

Planform Curvature Effects on Flutter Characteristics of a Wing With 56° Leading-Edge Sweep and Panel Aspect Ratio of 1.14

Donald F. Keller,
Maynard C. Sandford,
and Theresa L. Pinkerton

NASA

NASA
Technical
Paper
3116

1991

Planform Curvature Effects on Flutter Characteristics of a Wing With 56° Leading-Edge Sweep and Panel Aspect Ratio of 1.14

Donald F. Keller and Maynard C. Sandford
Langley Research Center
Hampton, Virginia

Theresa L. Pinkerton
University of Illinois
Urbana, Illinois

NASA
National Aeronautics and Space Administration
Office of Management
Scientific and Technical Information Program

Summary

An experimental and analytical investigation was initiated to determine the effects of planform curvature (curving the leading and trailing edges of a wing in the X-Y plane) on the transonic flutter characteristics of a series of three moderately swept wing models. The models were semispan cantilevered wings with a 3-percent biconvex airfoil and a panel aspect ratio of 1.14. The baseline model had straight leading and trailing edges (i.e., no planform curvature). The radii of curvature of the leading edges of the other two models were 200 and 80 in. The radius of curvature of the trailing edge for these two models was determined so that the planform area of each of the three models was 900 in^2. The wingspan, along with length and location of the root and tip chords, was identical for all three models.

Experimental flutter results were obtained in the Langley Transonic Dynamics Tunnel over a Mach number range from 0.60 to 1.00 with air as the test medium. All three models had a similar flutter behavior; no unusual flutter mechanisms were encountered. Experimental results showed that flutter-speed index and flutter frequency ratio increased as planform curvature increased (conversely, radius of curvature of the leading edge decreased) over the test range of Mach numbers.

Analytical flutter results were calculated for each of the models with unsteady aerodynamic subsonic kernel function theory. These are presented, along with experimental results, over a Mach number range from 0.60 to 0.95. The calculated flutter results corresponded well with the experimental data and showed that the first two natural vibrational modes (first bending and first torsion) were the primary modes coupling to produce flutter. Flutter analysis indicated that participation of the second mode in the flutter increased as planform curvature increased.

Introduction

Recently, long-range international air travel has increased significantly and will continue to increase well into the 21st century (ref. 1). This trend and advances in flight technologies, such as aircraft structures, materials, propulsion, and electronics, have resulted in a renewed interest in supersonic cruise aircraft, specifically the High Speed Civil Transport (HSCT) and the National Aero-Space Plane (NASP). As a result, NASA and several airframe manufacturers have developed new designs to meet the configuration requirements of a Mach 3+ HSCT (refs. 2 and 3). A sketch of a NASA HSCT concept currently being studied is shown in figure 1. A HSCT of this design would cruise at Mach 3.0, carry 250 passengers, and have a range of 6500 nautical miles (ref. 2). This concept involves curving the leading and trailing edges of the outboard portion of the wings in the X-Y plane. This feature is intended to improve aerodynamic performance by providing additional surface for the upper surface vortex (fig. 2) and to reduce the pitch-up instability associated with highly swept wings (ref. 4). An additional benefit shown by other studies is that wings with curved tips have better induced drag characteristics (refs. 5 and 6). Flutter, along with aerodynamic performance, is an important design consideration in the development of any HSCT configuration. Some earlier studies of planform and wingtip shapes and their effects on aerodynamic performance (refs. 7, 8, and 9) and flutter of generic wing configurations (refs. 10, 11, and 12) are presented in the literature. These studies showed that planform and wingtip shapes can have a significant effect on transonic flutter characteristics.

The present study was undertaken to investigate how planform curvature would affect the transonic flutter characteristics of a series of generic swept-wing models and to increase the available flutter data base related to planform and wingtip variations. The planforms of the three semispan cantilevered models used in this sensitivity study were based on the outboard portion of the recent NASA HSCT configuration. These simple models with a 3-percent-thick circular-arc airfoil shape were the same except for the radius of curvature of the leading and trailing edges. The baseline model had straight leading and trailing edges—i.e., no planform curvature—whereas the other two models had planform curvature. The moderately curved model most closely represented the wing planform shape of the NASA HSCT concept. The experimental transonic flutter boundaries presented in this report were obtained from a wind-tunnel test conducted in the Langley Transonic Dynamics Tunnel (TDT). The models were tested in air at an angle of attack of 0° and at Mach numbers ranging from 0.60 to 1.00.

A flutter analysis was performed with a subsonic kernel function flutter-prediction program. The purpose of the analysis was to evaluate the ability of this program to predict the effects of planform curvature and to provide a better understanding of the flutter characteristics of the models. The results of this analysis are presented along with the flutter results from the wind-tunnel test.

Symbols

b — reference length, root semichord, 1.667 ft c.g. center of gravity

f frequency, Hz

f_a analytical (calculated) natural frequency, Hz

f_f flutter frequency, Hz

f_f/f_2 flutter frequency ratio

f_m measured natural frequency, Hz

f_2 reference frequency, Hz

H total pressure, psf

M Mach number

m_o total model mass (minus mass of mounting tab), slugs

q dynamic pressure, psf

R_{LE} leading edge radius of curvature, in.

Re Reynolds number per ft

V_f flutter velocity, ft/s

V_I flutter-speed index, $\frac{V_f}{\omega_2 b(\mu^{1/2})}$

v_r reference volume of a conical frustum having wing root chord as base diameter, wingtip chord as upper diameter, and wing semispan as height, ft^3

x streamwise coordinate (positive downstream), in.

y spanwise coordinate (positive root to tip), in.

μ mass ratio, $m_o/\rho v_r$

ρ density, $slugs/ft^3$

ω_2 $= 2\pi f_2$, rad/sec

Test Apparatus

Wind Tunnel

The flutter test was conducted in the Langley Transonic Dynamics Tunnel (TDT). The TDT is a transonic wind tunnel designed specifically for the testing of aeroelastic models (ref. 13). The TDT is a continuous-flow, single-return, slotted-throat wind tunnel. The test section is 16-ft square with cropped corners. The tunnel is equipped to operate with air or a heavy gas (R-12) as the test medium. Air was used exclusively in the present study. Wind-tunnel speed and stagnation pressure are independently controllable from Mach numbers of near 0 to 1.20 and at pressures ranging from near 0 to 1 atm. The TDT operating envelope, with air as the test medium, is shown in figure 3. A unique safety feature of the TDT is a set of four quick-opening bypass valves that rapidly reduce the test-section Mach number and dynamic pressure when actuated. In the event of a model instability, such as flutter, these valves are used in an attempt to protect the wind-tunnel model. These capabilities make the TDT ideally suited for flutter testing.

Wind-Tunnel Model

The three semispan cantilevered wing models used in this study were based on the planform of the outboard portion of the wings of a recent NASA HSCT configuration. The planform shapes and dimensions for the three models are presented in figure 4. The baseline model had straight leading and trailing edges ($R_{LE} = \infty$) with sweeps of 56° and 37°, respectively, and a planform area of 900 in^2. The radii of curvature of the leading edges of the other two models were 200 and 80 in. The radius of curvature of the trailing edge of these two models was determined based on the same span, planform area, and root and tip chords of the baseline model. The span for each of the models was 32 in.

A photograph taken looking downstream at the moderately curved wing model ($R_{LE} = 200$ in.) mounted in the TDT is presented in figure 5. Each of the three models consisted of a 0.188-in-thick aluminum plate to which strips of balsa wood were bonded to provide the airfoil shape. The plate thickness was chosen to provide the correct stiffness for the models to flutter within the TDT air operating boundary. The balsa wood strips were bonded to the plate with the grain running parallel to the trailing edge of the baseline model and contoured to form a 3-percent-thick symmetric circular-arc airfoil section. The balsa wood was cut in the chordwise direction every 3 in. in span to minimize its effect on model stiffness (fig. 6). The models were mounted along the entire root chord by clamping the mounting tab between a steel plate and a steel beam which was attached to the sidewall turntable in the TDT. A splitter plate arrangement was used so that the model root chord was located outside the tunnel wall boundary layer. An angle-of-attack accelerometer located on the turntable was used to ensure that the models were at an angle of attack of 0°.

Model Instrumentation

Each model was instrumented with two strain-gauge bridges and an accelerometer. Their locations are shown in figure 6. The strain-gauge bridges were oriented to measure bending and torsion moments at the model root. The accelerometer was used to measure dynamic response near the wingtip. Instrumentation output was monitored on strip charts to assure safe margins for both static and dynamic loads and to aid in determining the onset of flutter.

Model Vibration Modes

Measured Modes

The first five natural frequencies were measured for each model mounted in the TDT. These measured natural frequencies are listed in table I. Hand raps at the root and wingtip were used to excite the models. Time-history signals from the strain-gauge bridges and accelerometer were input into a frequency analyzer to obtain model frequency spectrums. The effect of increasing the planform curvature was to lower the natural frequency of the second mode, whereas the first mode remained nearly constant.

Node line locations corresponding to the first four measured natural vibration modes were determined for each model mounted in the TDT. These node lines are presented in figure 7. An electromagnetic shaker was attached near the leading edge at the mid-span of the models to excite each natural vibration mode. A stationary reference accelerometer was attached to each wing near the tip where the maximum vibration amplitudes were expected for each vibration mode. A roving accelerometer was used to survey the vibration amplitudes across the entire upper surface of each model. The outputs of the two accelerometers were sent to a two-channel oscilloscope. A Lissajous figure, generated by the two signals, was monitored to detect phase shifts as the roving accelerometer passed across each node line. Increases in planform curvature had a significant effect on the location of node lines for the second, third, and fourth natural vibration modes.

Analytical Modes

Three finite element models representing the experimental models used in the present study were created and a dynamic structural analysis was performed with the MacNeal-Schwendler Corporation (MSC) NASTRAN finite element program (ref. 14). A complete listing of the three NASTRAN data decks used in this dynamic structural analysis is provided in the appendix. The analytical models consisted of 145 (baseline and R_{LE} = 200 in.) or 143 (R_{LE} = 80 in.) quadrilateral (CQUAD4) plate elements. These elements were chosen to model both the aluminum wing plate and the 3-percent-thick circular-arc balsa wood airfoil because they provide both membrane and bending stiffness. A layout of the NASTRAN finite element models is shown in figure 8. Elements representing balsa wood were superimposed on the elements representing the aluminum plate. Because of variations in the material properties of balsa wood, it was necessary to adjust the density and stiffness of these elements to obtain an analytical model more representative of the physical model. The density of the elements representing balsa wood was adjusted so that the mass of the finite element model was the same as that of the experimental model. The stiffness of these elements was then varied until the natural frequency of the second mode (reference mode) was approximately the same as for the experimental model. The analytical values for mass and center of gravity for the three models compared well with the measured values as shown in table I. Analytical frequencies and node lines for the models are presented with measured frequencies and node lines in table I and figure 7, respectively. The analytical natural frequencies and node line locations agreed well with the measured data for the three models.

The finite element analysis provided mode shapes and generalized masses which were used as input to the flutter analysis. The calculated mode shapes and natural frequencies for the three models are presented in figure 9.

Flutter Analysis

The Flutter Analysis System (FAST) computer program described in reference 15 was used to calculate flutter solutions. The flutter analysis was performed to provide a better understanding of model flutter mechanisms and to evaluate the ability of the program to predict planform curvature effects on flutter at Mach numbers between 0.60 and 0.95. The program uses a surface spline (ref. 16) to interpolate the displacements and slopes at the downwash collocation points from the calculated mode shapes. The number of collocation points was successively increased from 36 to 100. It was determined that using more than 64 (8×8) collocation points had little effect on the calculated flutter results. Figure 10 shows the Gaussian distribution of the 64 collocation points used in the flutter analysis. Next, the generalized unsteady aerodynamic forces are computed at each collocation point with subsonic kernel function theory (ref. 17). Flutter speeds are then calculated at various densities for a particular Mach number using an incremental damping approach (V-g method). From these calculations, a matched-point solution can be determined which gives the correct density and flutter frequency for a given flutter velocity. The use of this program should be limited to cases where only subsonic flow exists, because the program uses subsonic kernel function theory to calculate the generalized aerodynamic forces. The good agreement obtained above $M = 0.90$ between analytical and experimental data could be attributed to the thin airfoil section.

A FAST flutter analysis was performed for each of the three models. Since this method considers a wing to be a thin flat plate, the effects of the airfoil shape could not be modeled in the flutter analysis. Input to the analysis included the models' planform geometry, calculated mode shapes, calculated generalized masses, and the measured natural frequencies. Measured frequencies were used in the flutter analysis as an attempt to obtain more accurate flutter predictions. Both analytical and experimental results indicated that the first two vibration modes for the three models were the primary modes coupling to produce flutter. The first five vibration modes for each model were used in the flutter analysis. The use of additional modes had a negligible effect on the calculated flutter solutions. Matched-point flutter solutions were calculated for Mach numbers of 0.60, 0.80, 0.90, and 0.95. A typical structural damping value of 0.01 was used in the flutter analysis for each vibration mode.

Wind-Tunnel Test Procedure

The flutter boundaries were approached conservatively, and the Peak-Hold Spectrum method (ref. 18) was used to evaluate subcritical response data at various Mach number increments. The Peak-Hold Spectrum method involved analyzing frequency response data from the wing-mounted accelerometer and recording peak amplitudes for each dominant vibration frequency. Flutter projections were made based on plotted data of the inverse of the peak amplitudes versus tunnel dynamic pressure. The inverse amplitude should approach zero as the flutter condition is neared. It should be noted, however, that this was used only as a guideline in predicting the onset of flutter during testing. All flutter boundaries presented in this report consist of flutter points defined both visually and by monitoring dynamic response on a strip chart recorder. When flutter occurred, it was usually necessary to activate the tunnel bypass valves which would rapidly reduce the test-section dynamic pressure to a safe level before destructive wing deflections were encountered.

Figure 11 illustrates the tunnel operating procedure used to obtain the flutter boundaries presented in this paper. Generally, the first tunnel pass for a new configuration was intended to be free of flutter. After starting at a low stagnation pressure (100 to 200 psf), the tunnel Mach number and dynamic pressure were gradually increased by increasing the tunnel motor speed. The tunnel speed was increased until either a flutter condition was reached or a maximum test-section Mach number of 1.05 to 1.10 was obtained (see path 1, fig. 11). If no flutter was encountered, the test-section Mach number was reduced to a safe level and then held constant while the tunnel stagnation pressure was increased by 50 to 100 psf. Stagnation pressure was increased by bleeding additional air into the tunnel circuit. Again, the tunnel speed was gradually increased (see path 2, fig. 11). This procedure was repeated until the minimum flutter dynamic pressure was established. The same procedure was also used to define the remainder of the flutter boundary (see paths 3, 4, and 5, fig. 11).

Results and Discussion

The experimental and analytical flutter data are presented in tables II and III, respectively. These data tables include Mach number M, dynamic pressure q, flutter frequency f_f, flutter velocity V_f, density ρ, reference length b, mass ratio μ, flutter speed index V_I, Reynolds number Re, model mass m_o, reference frequency f_2, and flutter frequency ratio f_f/f_2, for each flutter point. The reference volume of the test medium v_r was 12.2 ft^3 for all three models. Flutter-speed index is a nondimensional velocity parameter, proportional to the square root of dynamic pressure. Flutter-speed index is frequently used to compare flutter results obtained for models with similar geometry and structural properties. Its use in the present study was to separate the small structural and geometric differences among the three models in an attempt to isolate the planform curvature effects on the flutter speed of the models.

Experimental and analytical flutter results are presented in figures 12 and 13. In figure 12, the results are shown in terms of dynamic pressure versus Mach number. In figure 13, the results are shown in terms of flutter-speed index, dynamic pressure, flutter frequency ratio, and mass ratio versus Mach number. These flutter boundaries represent neutral flutter stability. The three models had similar flutter behavior, and no unusual flutter mechanisms were encountered. The dominant vibration modes in the flutter mechanism were the first two modes. The dynamic motion for high transonic flutter points (M = 0.80 to 1.00) was dominated by the first mode (bending) of each model and was characterized by large wingtip deflections. The dynamic motion for flutter points in the lower transonic region (M = 0.60 to 0.80) involved coupling of the first and second modes and was characterized by both wingtip and mid-wing leading-edge deflections.

Experimental and analytical flutter dynamic pressure results for each of the models tested are presented in figure 12 for Mach numbers ranging from 0.60 to 0.99. The maximum tunnel operating paths at which no flutter was observed are included in the figures and indicate that the minimum dynamic pressure which produced flutter for all three models was near a Mach number of 1.00. The analytical results agreed well with the experimental results; the calculated boundaries were within 10 percent of the experimental results for Mach numbers from 0.60 to 0.95.

Experimental and analytical results showing the effects of planform curvature are presented in figure 13. These results include dynamic pressure, flutter-speed index, flutter frequency ratio, and mass ratio for test Mach number, ranging from 0.60 to 0.99. The experimental results show that the flutter dynamic pressure decreased approximately 20 percent for the moderately curved model (R_{LE} = 200 in.) when compared with that of the baseline model (no curvature) over the entire test Mach number range. However, the model with the greatest amount of planform curvature (R_{LE} = 80 in.) showed only a 10-percent decrease in flutter dynamic pressure near M = 0.60 and no change at M = 0.95. The experimental results showed an increase in flutter-speed index with increasing planform curvature over the test Mach number range. The flutter-speed index increased approximately 10 and 20 percent for the moderately curved wing and the most curved wing, respectively. The experimental flutter frequency ratio also increased with an increase in planform curvature, particularly in the lower transonic region. In addition, the flutter analysis indicated that the participation of the second mode in the flutter increased as planform curvature increased. The values for mass ratio, however, remained nearly constant with increases in planform curvature. The analytical results for dynamic pressure, flutter-speed index, flutter frequency ratio, and mass ratio agreed with the experimental results.

Summary of Results

The present study was undertaken to investigate the effects of planform curvature on the flutter characteristics of a generic 56° leading-edge swept-wing model with an aspect ratio of 1.14. This sensitivity study was developed to investigate the effects planform curvature might have on the flutter characteristics of a High Speed Civil Transport configuration and to expand the available flutter data base for planform variation studies. A series of three semispan, cantilevered models having different degrees of planform curvature were tested. The baseline model had straight leading and trailing edges with sweeps of 56° and 37°, respectively. The other two models had curved leading and trailing edges corresponding to different degrees of planform curvature. The experimental flutter results were obtained for test Mach numbers ranging from 0.60 to 1.00. In addition to a wind-tunnel test, a flutter analysis was performed with a subsonic, unsteady-aerodynamics flutter prediction program to evaluate the ability of the program to predict planform curvature effects and provide a better understanding of the flutter mechanisms. Both experimental and analytical flutter results are summarized as follows:

1. The three models had similar flutter behavior, and no unusual flutter mechanisms were encountered. Flutter points in the lower transonic region were dominated by both the first and second modes and were characterized by both wingtip and mid-wing leading-edge deflections. The higher transonic flutter points were dominated by the first mode of each model and were characterized by large wingtip deflections.

2. Flutter-speed index increased with increasing planform curvature over the test Mach number range. Compared with that for the baseline model, flutter-speed index increased approximately 10 and 20 percent for the moderately curved wing and the most curved wing, respectively. The experimental flutter dynamic pressure decreased 20 percent for the moderately curved model when compared with the baseline model (no curvature) over the entire test Mach number range. However, the model with the greatest amount of planform curvature showed only a 10-percent decrease in flutter dynamic pressure near a Mach number of 0.60 and no change at a Mach number of 0.95. The experimental flutter frequency ratio boundaries increased with each increase in planform curvature.

3. The analytical flutter results agreed well with the experimental data. The flutter analysis indicated that the flutter involved coupling of the first and second vibration modes and that the participation of the second vibration mode increased flutter as planform curvature increased.

NASA Langley Research Center
Hampton, VA 23665-5225
July 31, 1991

Appendix

MSC NASTRAN Finite Element Program, Version 65

This appendix presents the three data decks used in the dynamic analysis of the three models used in the present study. These finite element models were developed and the dynamic analysis completed using the MSC NASTRAN finite element program, Version 65. The finite element model for the baseline wing in figure A1 shows the typical layout and numbering of grid points and elements.

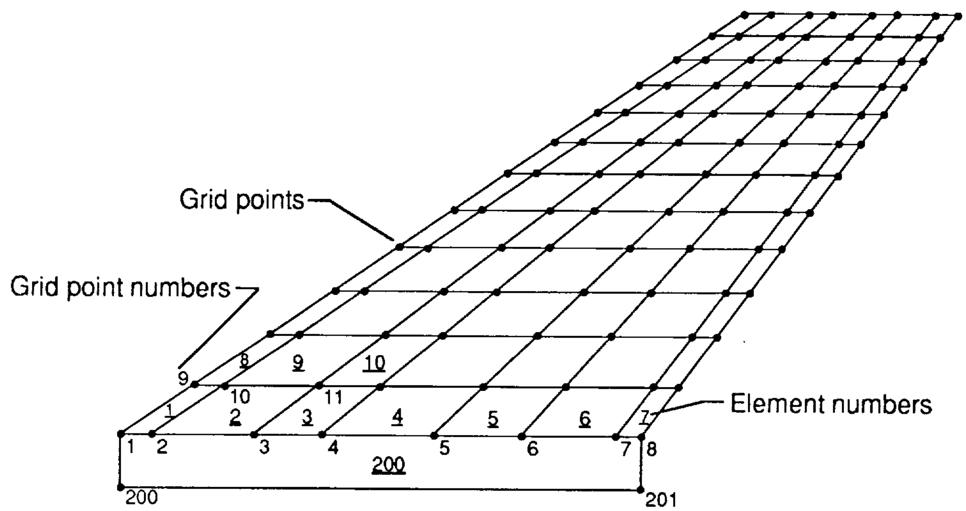

Figure A1. Typical layout of grid points and elements for NASTRAN finite element models.

1. NASTRAN DATA DECK FOR BASELINE MODEL

```
ID, NO CURVATURE,CURVED PANEL STUDY,T=.118,BALSA LAYOUT INCLUDED
SOL 3
TIME 100
CEND
$CASE CONTROL DECK
TITLE=CURVED PANEL FLUTTER STUDY,NO CURVED MODEL, T=.118,BALSA LAYOUT
SUBTITLE= QUAD4 ELEMENTS, BALSA
ECHO=BOTH
DISP=ALL
METHOD=10
PLOTID=BLDG. 648,DFK,CURVED STUDY,T=.118,BALSA
LINE=35
OUTPUT(PLOT)
PLOTTER NAST
SET 1=ALL
SET 2=102 THRU 183
$FIRST PLOT
AXES Z,X,Y
VIEW 0.,0.,0.
FIND SCALE, ORIGIN 1, SET 1
PLOT SET 1, ORIGIN 1
AXES X,Y,Z
VIEW 124.,35.,0.
FIND SCALE,ORIGIN 1,SET 1
```

```
PLOT MODAL DEFO 0,SET 1
AXES Z,X,Y
VIEW 0.,0.,0.
FIND SCALE,ORIGIN 1,SET 2
PLOT SET 2,ORIGIN 1,LABEL ELEMENTS
BEGIN BULK
$TAB
GRID,200,,0.,-4.,0.
GRID,201,,40.,-4.,0.
CQUAD4,200,20,200,201,8,1
$GRID POINT DEFINITION
GRID,1,,0.,0.,,,123456
=,2,,2.0,0.,,,123456
=,3,,9.6,0.,,,123456
=,4,,16.,0.,,,123456
=,5,,24.,0.,,,123456
=,6,,30.4,0.,,,123456
=,7,,38.0,0.,,,123456
=,8,,40.,0.,,,123456
=,9,,5.82,3.9
=,10,,7.82,=
=,11,,14.8,=
=,12,,20.7,=
=,13,,28.1,=
=,14,,33.9,=
=,15,,40.9,=
=,16,,42.93,=
=,17,,11.57,7.75
=,18,,13.57,=
=,19,,20.0,=
=,20,,25.3,=
=,21,,32.1,=
=,22,,37.4,=
=,23,,43.8,=
=,24,,45.81,=
=,25,,16.42,11.0
=,26,,18.42,=
=,27,,24.4,=
=,28,,29.1,=
=,29,,35.5,=
=,30,,40.3,=
=,31,,46.25,=
=,32,,48.25,=
=,33,,21.34,14.3
=,34,,23.3,=
=,35,,28.8,=
=,36,,33.1,=
=,37,,39.0,=
=,38,,43.3,=
=,39,,48.7,=
=,40,,50.73,=
=,41,,25.52,17.1
=,42,,27.5,=
=,43,,32.6,=
=,44,,36.4,=
```

```
=,45,,41.9,=
=,46,,45.8,=
=,47,,50.8,=
=,48,,52.83,=
=,49,,29.55,19.8
=,50,,31.55,=
=,51,,36.2,=
=,52,,39.7,=
=,53,,44.7,=
=,54,,48.2,=
=,55,,52.9,=
=,56,,54.85,=
=,57,,33.14,22.2
=,58,,35.1,=
=,59,,39.4,=
=,60,,42.5,=
=,61,,47.2,=
=,62,,50.4,=
=,63,,54.65,=
=,64,,56.65,=
=,65,,36.57,24.5
=,66,,38.6,=
=,67,,42.5,=
=,68,,45.3,=
=,69,,49.6,=
=,70,,52.5,=
=,71,,56.4,=
=,72,,58.38,=
=,73,,39.56,26.5
=,74,,41.6,=
=,75,,45.2,=
=,76,,47.7,=
=,77,,51.7,=
=,78,,54.3,=
=,79,,57.9,=
=,80,,59.88,=
=,81,,42.54,28.5
=,82,,44.5,=
=,83,,47.9,=
=,84,,50.1,=
=,85,,53.8,=
=,86,,56.1,=
=,87,,59.4,=
=,88,,61.38,=
=,89,,45.23,30.3
=,90,,47.2,=
=,91,,50.3,=
=,92,,52.2,=
=,93,,55.7,=
=,94,,57.7,=
=,95,,60.7,=
=,96,,62.73,=
=,97,,47.75,32.
=,98,,49.80,=
=,99,,52.6,=
```

```
=,100,,54.25,=
=,101,,57.5,=
=,102,,59.2,=
=,103,,62.0,=
=,104,,64.0,=
$BEGIN ELEMENT DEFINITION FOR ALUMINUM PLATE
CQUAD4,1,20,1,2,10,9,,,+C1
=,2,20,2,3,11,10
=,3,20,3,4,12,11
=,4,20,4,5,13,12
=,5,=,5,6,14,13
=,6,=,6,7,15,14
=,7,=,7,8,16,15,,,+C7
=,8,=,9,10,18,17,,,+C8
=,9,=,10,11,19,18
=,10,=,11,12,20,19
=,11,=,12,13,21,20
=,12,=,13,14,22,21
=,13,=,14,15,23,22
=,14,=,15,16,24,23,,,+C14
=,15,=,17,18,26,25,,,+C15
=,16,=,18,19,27,26
=,17,=,19,20,28,27
=,18,=,20,21,29,28
=,19,=,21,22,30,29
=,20,=,22,23,31,30
=,21,=,23,24,32,31,,,+C21
=,22,=,25,26,34,33,,,+C22
=,23,=,26,27,35,34
=,24,=,27,28,36,35
=,25,=,28,29,37,36
=,26,=,29,30,38,37
=,27,=,30,31,39,38
=,28,=,31,32,40,39,,,+C28
=,29,=,33,34,42,41,,,+C29
=,30,=,34,35,43,42
=,31,=,35,36,44,43
=,32,=,36,37,45,44
=,33,=,37,38,46,45
=,34,=,38,39,47,46
=,35,=,39,40,48,47,,,+C35
=,36,=,41,42,50,49,,,+C36
=,37,=,42,43,51,50
=,38,=,43,44,52,51
=,39,=,44,45,53,52
=,40,=,45,46,54,53
=,41,=,46,47,55,54
=,42,=,47,48,56,55,,,+C42
=,43,=,49,50,58,57,,,+C43
=,44,=,50,51,59,58
=,45,=,51,52,60,59
=,46,=,52,53,61,60
=,47,=,53,54,62,61
=,48,=,54,55,63,62
=,49,=,55,56,64,63,,,+C49
```

```
=,50,=,57,58,66,65,,,+C50
=,51,=,58,59,67,66
=,52,=,59,60,68,67
=,53,=,60,61,69,68
=,54,=,61,62,70,69
=,55,=,62,63,71,70
=,56,=,63,64,72,71,,,+C56
=,57,=,65,66,74,73,,,+C57
=,58,=,66,67,75,74
=,59,=,67,68,76,75
=,60,=,68,69,77,76
=,61,=,69,70,78,77
=,62,=,70,71,79,78
=,63,=,71,72,80,79,,,+C63
=,64,=,73,74,82,81,,,+C64
=,65,=,74,75,83,82
=,66,=,75,76,84,83
=,67,=,76,77,85,84
=,68,=,77,78,86,85
=,69,=,78,79,87,86
=,70,=,79,80,88,87,,,+C70
=,71,=,81,82,90,89,,,+C71
=,72,=,82,83,91,90
=,73,=,83,84,92,91
=,74,=,84,85,93,92
=,75,=,85,86,94,93
=,76,=,86,87,95,94
=,77,=,87,88,96,95,,,+C77
=,78,=,89,90,98,97,,,+C78
=,79,=,90,91,99,98
=,80,=,91,92,100,99
=,81,=,92,93,101,100
=,82,=,93,94,102,101
=,83,=,94,95,103,102
=,84,=,95,96,104,103,,,+C84
$ CONTINUATION CARDS FOR ALUMINUM ELEMNTS(THICKNESS)
+C1,,,0.,,,0.
+C8,,,=,,,=
+C15,,,=,,,=
+C22,,,=,,,=
+C29,,,=,,,=
+C36,,,=,,,=
+C43,,,=,,,=
+C50,,,=,,,=
+C57,,,=,,,=
+C64,,,=,,,=
+C71,,,=,,,=
+C78,,,=,,,=
+C7,,,,0.,0.,
+C14,,,,=,=
+C21,,,,=,=
+C28,,,,=,=
+C35,,,,=,=
+C42,,,,=,=
+C49,,,,=,=
```

```
+C56,,,,=,=
+C63,,,,=,=
+C70,,,,=,=
+C77,,,,=,=
+C84,,,,=,=
$BALSA ELEMENTS AND CONT. CARDS
CQUAD4,102,50,2,3,11,10,,,+C102
=,103,50,3,4,12,11,,,+C103
=,104,50,4,5,13,12,,,+C104
=,105,=,5,6,14,13,,,+C105
=,106,=,6,7,15,14,,,+C106
=,109,=,10,11,19,18,,,+C109
=,110,=,11,12,20,19,,,+C110
=,111,=,12,13,21,20,,,+C111
=,112,=,13,14,22,21,,,+C112
=,113,=,14,15,23,22,,,+C113
=,116,=,18,19,27,26,,,+C116
=,117,=,19,20,28,27,,,+C117
=,118,=,20,21,29,28,,,+C118
=,119,=,21,22,30,29,,,+C119
=,120,=,22,23,31,30,,,+C120
=,123,=,26,27,35,34,,,+C123
=,124,=,27,28,36,35,,,+C124
=,125,=,28,29,37,36,,,+C125
=,126,=,29,30,38,37,,,+C126
=,127,=,30,31,39,38,,,+C127
=,130,=,34,35,43,42,,,+C130
=,131,=,35,36,44,43,,,+C131
=,132,=,36,37,45,44,,,+C132
=,133,=,37,38,46,45,,,+C133
=,134,=,38,39,47,46,,,+C134
=,137,=,42,43,51,50,,,+C137
=,138,=,43,44,52,51,,,+C138
=,139,=,44,45,53,52,,,+C139
=,140,=,45,46,54,53,,,+C140
=,141,=,46,47,55,54,,,+C141
=,144,=,50,51,59,58,,,+C144
=,145,=,51,52,60,59,,,+C145
=,146,=,52,53,61,60,,,+C146
=,147,=,53,54,62,61,,,+C147
=,148,=,54,55,63,62,,,+C148
=,151,=,58,59,67,66,,,+C151
=,152,=,59,60,68,67,,,+C152
=,153,=,60,61,69,68,,,+C153
=,154,=,61,62,70,69,,,+C154
=,155,=,62,63,71,70,,,+C155
=,158,=,66,67,75,74,,,+C158
=,159,=,67,68,76,75,,,+C159
=,160,=,68,69,77,76,,,+C160
=,161,=,69,70,78,77,,,+C161
=,162,=,70,71,79,78,,,+C162
=,165,=,74,75,83,82,,,+C165
=,166,=,75,76,84,83,,,+C166
=,167,=,76,77,85,84,,,+C167
=,168,=,77,78,86,85,,,+C168
```

```
=,169,=,78,79,87,86,,,+C169
=,172,=,82,83,91,90,,,+C172
=,173,=,83,84,92,91,,,+C173
=,174,=,84,85,93,92,,,+C174
=,175,=,85,86,94,93,,,+C175
=,176,=,86,87,95,94,,,+C176
=,179,=,90,91,99,98,,,+C179
=,180,=,91,92,100,99,,,+C180
=,181,=,92,93,101,100,,,+C181
=,182,=,93,94,102,101,,,+C182
=,183,=,94,95,103,102,,,+C183
+C102,,,.00,0.69,0.63,.00
+C103,,,.69,.96,.88,.63
+C104,,,.96,.96,.88,.88
+C105,,,.96,.69,.63,.88
+C106,,,.690,0.,0.,.630
+C109,,,.00,.63,.5700,0.
+C110,,,.63,.88,.80,.57
+C111,,,.88,.88,.80,.80
+C112,,,.88,.63,.57,.80
+C113,,,.630,0.,0.,.570
+C116,,,.00,.570,.530,0.
+C117,,,.57,.80,.73,.53
+C118,,,.80,.80,.73,.73
+C119,,,.80,.57,.53,.73
+C120,,,.570,0.,0.,.530
+C123,,,.00,.530,.480,0.
+C124,,,.53,.73,.66,.48
+C125,,,.73,.73,.66,.66
+C126,,,.73,.53,.48,.66
+C127,,,.530,0.,0.,.480
+C130,,,.00,.480,.440,0.
+C131,,,.48,.66,.60,.44
+C132,,,.66,.66,.60,.60
+C133,,,.66,.48,.44,.60
+C134,,,.480,0.,0.,.440
+C137,,,.00,.440,.40,0.
+C138,,,.44,.60,.54,.40
+C139,,,.60,.60,.54,.54
+C140,,,.60,.44,.40,.54
+C141,,,.440,0.,0.,.400
+C144,,,.00,.40,.36,.00
+C145,,,.40,.54,.49,.36
+C146,,,.54,.54,.49,.49
+C147,,,.54,.40,.36,.49
+C148,,,.40,.00,.00,.36
+C151,,,.00,.36,.33,.00
+C152,,,.36,.49,.44,.33
+C153,,,.49,.49,.44,.44
+C154,,,.49,.36,.33,.44
+C155,,,.36,.00,.00,.330
+C158,,,.00,.33,.30,.00
+C159,,,.33,.44,.40,.30
+C160,,,.44,.44,.40,.40
+C161,,,.44,.33,.30,.40
```

```
+C162,,,.33,.00,.00,.30
+C165,,,.00,.30,.27,.00
+C166,,,.30,.40,.36,.27
+C167,,,.40,.40,.36,.36
+C168,,,.40,.30,.27,.36
+C169,,,.30,.00,.00,.27
+C172,,,.00,.27,.24,.00
+C173,,,.27,.36,.32,.24
+C174,,,.36,.36,.32,.32
+C175,,,.36,.27,.24,.32
+C176,,,.27,0.,0.,.24
+C179,,,.00,.24,.22,.00
+C180,,,.24,.32,.28,.22
+C181,,,.32,.32,.28,.28
+C182,,,.32,.24,.22,.28
+C183,,,.24,.00,.00,.22
$MAT PROP. ID
PSHELL,20,30,.188,30,,30,,0.
MAT1,30,1.05+7,,.3334,.000262
PSHELL,50,60,1.+7,60,,60,,0.
MAT1,60,2.70+5,,.05,2.50-5
EIGR,10,SINV,.1,100.,,,,,+EIGR
+EIGR,MAX
PARAM,GRDPNT,1
ENDDATA
```

2. NASTRAN DATA DECK FOR MODERATELY CURVED MODEL (R_{LE}=200 IN.)

```
ID, R=200,CURVED PANEL STUDY,T=.118,BALSA LAYOUT
SOL 3
TIME 150
CEND
$CASE CONTROL DECK
TITLE=CURVED PANEL FLUTTER STUDY, R200, T=.118,BALSA LAYOUT
SUBTITLE= QUAD4 ELEMENTS, BALSA, 3% AIRFOIL
ECHO=BOTH
DISP=ALL
METHOD=10
PLOTID=BLDG. 648,DFK,CURVED STUDY,T=.118,BALSA,3% AIRFOIL
LINE=35
OUTPUT(PLOT)
PLOTTER NAST
SET 1=ALL
SET 2=102 THRU 183
$FIRST PLOT
AXES Z,X,Y
VIEW 0.,0.,0.
FIND SCALE, ORIGIN 1, SET 1
PLOT SET 1, ORIGIN 1
AXES X,Y,Z
VIEW 124.,35.,0.
FIND SCALE,ORIGIN 1,SET 1
PLOT MODAL DEFO 0,SET 1
AXES Z,X,Y
VIEW 0.,0.,0.
FIND SCALE,ORIGIN 1,SET 2
```

```
PLOT SET 2,ORIGIN 1
BEGIN BULK
$TAB
GRID,200,,0.,-4.,0.
GRID,201,,40.,-4.,0.
CQUAD4,200,20,200,201,8,1
GRID,1,,0.,0.,,,123456
=,2,,2.0,0.,,,123456
=,3,,9.8,0.,,,123456
=,4,,16.6,0.,,,123456
=,5,,23.4,0.,,,123456
=,6,,30.2,0.,,,123456
=,7,,38.0,0.,,,123456
=,8,,40.,0.,,,123456
=,9,,4.56,3.9
=,10,,6.56,=
=,11,,13.8,=
=,12,,20.0,=
=,13,,26.2,=
=,14,,32.5,=
=,15,,39.7,=
=,16,,41.69,=
=,17,,9.110,7.75
=,18,,11.11,=
=,19,,17.8,=
=,20,,23.4,=
=,21,,29.1,=
=,22,,34.7,=
=,23,,41.4,=
=,24,,43.37,=
=,25,,13.58,11.0
=,26,,15.58,=
=,27,,21.7,=
=,28,,26.9,=
=,29,,32.0,=
=,30,,37.2,=
=,31,,43.3,=
=,32,,45.34,=
=,33,,18.05,14.3
=,34,,20.05,=
=,35,,25.7,=
=,36,,30.4,=
=,37,,35.0,=
=,38,,39.7,=
=,39,,45.3,=
=,40,,47.31,=
=,41,,21.97,17.1
=,42,,24.0,=
=,43,,29.2,=
=,44,,33.5,=
=,45,,37.8,=
=,46,,42.0,=
=,47,,47.3,=
=,48,,49.29,=
=,49,,25.88,19.8
```

```
=,50,,27.9,=
=,51,,32.7,=
=,52,,36.6,=
=,53,,40.5,=
=,54,,44.3,=
=,55,,49.2,=
=,56,,51.19,=
=,57,,29.72,22.2
=,58,,31.7,=
=,59,,36.2,=
=,60,,39.7,=
=,61,,43.3,=
=,62,,46.8,=
=,63,,51.3,=
=,64,,53.28,=
=,65,,33.56,24.5
=,66,,35.56,=
=,67,,39.7,=
=,68,,42.9,=
=,69,,46.0,=
=,70,,49.2,=
=,71,,53.4,=
=,72,,55.37,=
=,73,,37.18,26.5
=,74,,39.18,=
=,75,,43.0,=
=,76,,45.9,=
=,77,,48.8,=
=,78,,51.6,=
=,79,,55.5,=
=,80,,57.49,=
=,81,,40.79,28.5
=,82,,42.8,=
=,83,,46.4,=
=,84,,48.9,=
=,85,,51.5,=
=,86,,54.0,=
=,87,,57.6,=
=,88,,59.61,=
=,89,,44.27,30.3
=,90,,46.3,=
=,91,,49.6,=
=,92,,51.9,=
=,93,,54.2,=
=,94,,56.5,=
=,95,,59.8,=
=,96,,61.81,=
=,97,,47.75,32.
=,98,,49.75,=
=,99,,52.8,=
=,100,,54.90,=
=,101,,56.9,=
=,102,,59.0,=
=,103,,62.0,=
=,104,,64.0,=
```

```
$BEGIN ELEMENT DEFINITION
CQUAD4,1,20,1,2,10,9,,,+C1
=,2,20,2,3,11,10
=,3,20,3,4,12,11
=,4,20,4,5,13,12
=,5,=,5,6,14,13
=,6,=,6,7,15,14
=,7,=,7,8,16,15,,,+C7
=,8,=,9,10,18,17,,,+C8
=,9,=,10,11,19,18
=,10,=,11,12,20,19
=,11,=,12,13,21,20
=,12,=,13,14,22,21
=,13,=,14,15,23,22
=,14,=,15,16,24,23,,,+C14
=,15,=,17,18,26,25,,,+C15
=,16,=,18,19,27,26
=,17,=,19,20,28,27
=,18,=,20,21,29,28
=,19,=,21,22,30,29
=,20,=,22,23,31,30
=,21,=,23,24,32,31,,,+C21
=,22,=,25,26,34,33,,,+C22
=,23,=,26,27,35,34
=,24,=,27,28,36,35
=,25,=,28,29,37,36
=,26,=,29,30,38,37
=,27,=,30,31,39,38
=,28,=,31,32,40,39,,,+C28
=,29,=,33,34,42,41,,,+C29
=,30,=,34,35,43,42
=,31,=,35,36,44,43
=,32,=,36,37,45,44
=,33,=,37,38,46,45
=,34,=,38,39,47,46
=,35,=,39,40,48,47,,,+C35
=,36,=,41,42,50,49,,,+C36
=,37,=,42,43,51,50
=,38,=,43,44,52,51
=,39,=,44,45,53,52
=,40,=,45,46,54,53
=,41,=,46,47,55,54
=,42,=,47,48,56,55,,,+C42
=,43,=,49,50,58,57,,,+C43
=,44,=,50,51,59,58
=,45,=,51,52,60,59
=,46,=,52,53,61,60
=,47,=,53,54,62,61
=,48,=,54,55,63,62
=,49,=,55,56,64,63,,,+C49
=,50,=,57,58,66,65,,,+C50
=,51,=,58,59,67,66
=,52,=,59,60,68,67
=,53,=,60,61,69,68
=,54,=,61,62,70,69
```

```
=,55,=,62,63,71,70
=,56,=,63,64,72,71,,,+C56
=,57,=,65,66,74,73,,,+C57
=,58,=,66,67,75,74
=,59,=,67,68,76,75
=,60,=,68,69,77,76
=,61,=,69,70,78,77
=,62,=,70,71,79,78
=,63,=,71,72,80,79,,,+C63
=,64,=,73,74,82,81,,,+C64
=,65,=,74,75,83,82
=,66,=,75,76,84,83
=,67,=,76,77,85,84
=,68,=,77,78,86,85
=,69,=,78,79,87,86
=,70,=,79,80,88,87,,,+C70
=,71,=,81,82,90,89,,,+C71
=,72,=,82,83,91,90
=,73,=,83,84,92,91
=,74,=,84,85,93,92
=,75,=,85,86,94,93
=,76,=,86,87,95,94
=,77,=,87,88,96,95,,,+C77
=,78,=,89,90,98,97,,,+C78
=,79,=,90,91,99,98
=,80,=,91,92,100,99
=,81,=,92,93,101,100
=,82,=,93,94,102,101
=,83,=,94,95,103,102
=,84,=,95,96,104,103,,,+C84
$ CONTINUATION CARDS (THICKNESS)
+C1,,,0.,,,0.
+C8,,,=,,,=
+C15,,,=,,,=
+C22,,,=,,,=
+C29,,,=,,,=
+C36,,,=,,,=
+C43,,,=,,,=
+C50,,,=,,,=
+C57,,,=,,,=
+C64,,,=,,,=
+C71,,,=,,,=
+C78,,,=,,,=
+C7,,,,0.,0.,
+C14,,,,=,=
+C21,,,,=,=
+C28,,,,=,=
+C35,,,,=,=
+C42,,,,=,=
+C49,,,,=,=
+C56,,,,=,=
+C63,,,,=,=
+C70,,,,=,=
+C77,,,,=,=
+C84,,,,=,=
```

```
$BALSA ELEMENTS AND CONT. CARDS
CQUAD4,102,50,2,3,11,10,,,+C102
=,103,50,3,4,12,11,,,+C103
=,104,50,4,5,13,12,,,+C104
=,105,=,5,6,14,13,,,+C105
=,106,=,6,7,15,14,,,+C106
=,109,=,10,11,19,18,,,+C109
=,110,=,11,12,20,19,,,+C110
=,111,=,12,13,21,20,,,+C111
=,112,=,13,14,22,21,,,+C112
=,113,=,14,15,23,22,,,+C113
=,116,=,18,19,27,26,,,+C116
=,117,=,19,20,28,27,,,+C117
=,118,=,20,21,29,28,,,+C118
=,119,=,21,22,30,29,,,+C119
=,120,=,22,23,31,30,,,+C120
=,123,=,26,27,35,34,,,+C123
=,124,=,27,28,36,35,,,+C124
=,125,=,28,29,37,36,,,+C125
=,126,=,29,30,38,37,,,+C126
=,127,=,30,31,39,38,,,+C127
=,130,=,34,35,43,42,,,+C130
=,131,=,35,36,44,43,,,+C131
=,132,=,36,37,45,44,,,+C132
=,133,=,37,38,46,45,,,+C133
=,134,=,38,39,47,46,,,+C134
=,137,=,42,43,51,50,,,+C137
=,138,=,43,44,52,51,,,+C138
=,139,=,44,45,53,52,,,+C139
=,140,=,45,46,54,53,,,+C140
=,141,=,46,47,55,54,,,+C141
=,144,=,50,51,59,58,,,+C144
=,145,=,51,52,60,59,,,+C145
=,146,=,52,53,61,60,,,+C146
=,147,=,53,54,62,61,,,+C147
=,148,=,54,55,63,62,,,+C148
=,151,=,58,59,67,66,,,+C151
=,152,=,59,60,68,67,,,+C152
=,153,=,60,61,69,68,,,+C153
=,154,=,61,62,70,69,,,+C154
=,155,=,62,63,71,70,,,+C155
=,158,=,66,67,75,74,,,+C158
=,159,=,67,68,76,75,,,+C159
=,160,=,68,69,77,76,,,+C160
=,161,=,69,70,78,77,,,+C161
=,162,=,70,71,79,78,,,+C162
=,165,=,74,75,83,82,,,+C165
=,166,=,75,76,84,83,,,+C166
=,167,=,76,77,85,84,,,+C167
=,168,=,77,78,86,85,,,+C168
=,169,=,78,79,87,86,,,+C169
=,172,=,82,83,91,90,,,+C172
=,173,=,83,84,92,91,,,+C173
=,174,=,84,85,93,92,,,+C174
=,175,=,85,86,94,93,,,+C175
```

```
=,176,=,86,87,95,94,,,+C176
=,179,=,90,91,99,98,,,+C179
=,180,=,91,92,100,99,,,+C180
=,181,=,92,93,101,100,,,+C181
=,182,=,93,94,102,101,,,+C182
=,183,=,94,95,103,102,,,+C183
+C102,,,.00,0.69,0.63,.00
+C103,,,.69,.96,.88,.63
+C104,,,.96,.96,.88,.88
+C105,,,.96,.69,.63,.88
+C106,,,.690,0.,0.,.630
+C109,,,.00,.63,.5700,0.
+C110,,,.63,.88,.80,.57
+C111,,,.88,.88,.80,.80
+C112,,,.88,.63,.57,.80
+C113,,,.630,0.,0.,.570
+C116,,,.00,.570,.530,0.
+C117,,,.57,.80,.73,.53
+C118,,,.80,.80,.73,.73
+C119,,,.80,.57,.53,.73
+C120,,,.570,0.,0.,.530
+C123,,,.00,.530,.480,0.
+C124,,,.53,.73,.66,.48
+C125,,,.73,.73,.66,.66
+C126,,,.73,.53,.48,.66
+C127,,,.530,0.,0.,.480
+C130,,,.00,.480,.440,0.
+C131,,,.48,.66,.60,.44
+C132,,,.66,.66,.60,.60
+C133,,,.66,.48,.44,.60
+C134,,,.480,0.,0.,.440
+C137,,,.00,.440,.40,0.
+C138,,,.44,.60,.54,.40
+C139,,,.60,.60,.54,.54
+C140,,,.60,.44,.40,.54
+C141,,,.440,0.,0.,.400
+C144,,,.00,.40,.36,.00
+C145,,,.40,.54,.49,.36
+C146,,,.54,.54,.49,.49
+C147,,,.54,.40,.36,.49
+C148,,,.40,.00,.00,.36
+C151,,,.00,.36,.33,.00
+C152,,,.36,.49,.44,.33
+C153,,,.49,.49,.44,.44
+C154,,,.49,.36,.33,.44
+C155,,,.36,.00,.00,.330
+C158,,,.00,.33,.30,.00
+C159,,,.33,.44,.40,.30
+C160,,,.44,.44,.40,.40
+C161,,,.44,.33,.30,.40
+C162,,,.33,.00,.00,.30
+C165,,,.00,.30,.27,.00
+C166,,,.30,.40,.36,.27
+C167,,,.40,.40,.36,.36
+C168,,,.40,.30,.27,.36
```

```
+C169,,,.30,.00,.00,.27
+C172,,,.00,.27,.24,.00
+C173,,,.27,.36,.32,.24
+C174,,,.36,.36,.32,.32
+C175,,,.36,.27,.24,.32
+C176,,,.27,0.,0.,.24
+C179,,,.00,.24,.22,.00
+C180,,,.24,.32,.28,.22
+C181,,,.32,.32,.28,.28
+C182,,,.32,.24,.22,.28
+C183,,,.24,.00,.00,.22
$MAT PROP. ID
PSHELL,20,30,.188,30,,30,,0.
MAT1,30,1.05+7,,.3334,.000262
PSHELL,50,60,1.+7,60,,60,,0.
MAT1,60,1.6+5,,.05,1.5460-5
EIGR,10,SINV,.1,80.0,,,,,+EIGR
+EIGR,MAX
PARAM,GRDPNT,1
ENDDATA
```

3. NASTRAN DATA DECK FOR MOST CURVED MODEL (R_{LE}=80 IN.)

```
ID,R=80,CURVED PANEL STUDY,T=.118,BALSA LAYOUT,3% AIRFOIL
SOL 3
TIME 100
CEND
$CASE CONTROL DECK
TITLE=CURVED PANEL FLUTTER STUDY,R=80, T=.118,BALSA LAYOUT
SUBTITLE= QUAD4 ELEMENTS, BALSA,3% AIRFOIL
ECHO=BOTH
DISP=ALL
METHOD=10
PLOTID=BLDG. 648,DFK,CURVED STUDY,T=.118
LINE=35
OUTPUT(PLOT)
PLOTTER NAST
SET 1=ALL
SET 2=102 THRU 182
$FIRST PLOT
AXES Z,X,Y
VIEW 0.,0.,0.
FIND SCALE, ORIGIN 1, SET 1
PLOT SET 1, ORIGIN 1
AXES X,Y,Z
VIEW 124.,35.,0.
FIND SCALE,ORIGIN 1,SET 1
PLOT MODAL DEFO 0,SET 1
AXES Z,X,Y
VIEW 0.,0.,0.
FIND SCALE,ORIGIN 1,SET 2
PLOT SET 2,ORIGIN 1
BEGIN BULK
GRID,200,,0.,-4.,0.
GRID,201,,40.,-4.,0.
CQUAD4,200,20,200,201,8,1
```

```
GRID,1,,0.,0.,,,123456
=,2,,2.0,0.,,,123456
=,3,,9.2,0.,,,123456
=,4,,16.4,0.,,,123456
=,5,,23.6,0.,,,123456
=,6,,30.8,0.,,,123456
=,7,,38.0,0.,,,123456
=,8,,40.,0.,,,123456
=,9,,3.10,3.9
=,10,,5.10,=
=,11,,11.7,=
=,12,,18.3,=
=,13,,25.0,=
=,14,,31.6,=
=,15,,38.2,=
=,16,,40.20,=
=,17,,6.200,7.75
=,18,,8.20,=
=,19,,14.2,=
=,20,,20.3,=
=,21,,26.3,=
=,22,,32.4,=
=,23,,38.4,=
=,24,,40.41,=
=,25,,9.660,11.0
=,26,,11.66,=
=,27,,17.2,=
=,28,,22.8,=
=,29,,28.3,=
=,30,,33.9,=
=,31,,39.4,=
=,32,,41.44,=
=,33,,13.12,14.3
=,34,,15.12,=
=,35,,20.2,=
=,36,,25.3,=
=,37,,30.3,=
=,38,,35.4,=
=,39,,40.5,=
=,40,,42.47,=
=,41,,16.54,17.1
=,42,,18.6,=
=,43,,23.3,=
=,44,,27.9,=
=,45,,32.6,=
=,46,,37.3,=
=,47,,41.97,=
=,48,,43.97,=
=,49,,19.97,19.8
=,50,,21.97,=
=,51,,26.3,=4
=,52,,30.6,=
=,53,,34.9,=
=,54,,39.2,=
=,55,,43.5,=
```

```
=,56,,45.47,=
=,57,,23.82,22.2
=,58,,25.8,=
=,59,,29.7,=
=,60,,33.7,=
=,61,,37.6,=
=,62,,41.6,=
=,63,,45.52,=
=,64,,47.52,=
=,65,,27.66,24.5
=,66,,29.7,=
=,67,,33.3,=
=,68,,36.9,=
=,69,,40.4,=
=,70,,44.0,=
=,71,,47.6,=
=,72,,49.57,=
=,73,,32.00,26.5
=,74,,34.0,=
=,75,,37.3,=
=,76,,40.5,=
=,77,,43.8,=
=,78,,47.0,=
=,79,,50.3,=
=,80,,52.26,=
=,81,,36.34,28.5
=,82,,38.3,=
=,83,,41.3,=
=,84,,44.2,=
=,85,,47.1,=
=,86,,50.0,=
=,87,,52.9,=
=,88,,54.94,=
=,89,,42.04,30.3
=,90,,44.0,=
=,91,,47.4,=
=,92,,50.8,=
=,93,,54.1,=
=,94,,57.5,=
=,95,,59.47,=
=,96,,47.75,32.0
=,97,,49.75,32.
=,98,,52.80,=
=,99,,55.9,=
=,100,,58.90,=
=,101,,62.0,=
=,102,,64.0,=
$BEGIN ELEMENT DEFINITION
CQUAD4,1,20,1,2,10,9,,,+C1
=,2,20,2,3,11,10
=,3,20,3,4,12,11
=,4,20,4,5,13,12
=,5,=,5,6,14,13
=,6,=,6,7,15,14
=,7,=,7,8,16,15,,,+C7
```

```
=,8,=,9,10,18,17,,,+C8
=,9,=,10,11,19,18
=,10,=,11,12,20,19
=,11,=,12,13,21,20
=,12,=,13,14,22,21
=,13,=,14,15,23,22
=,14,=,15,16,24,23,,,+C14
=,15,=,17,18,26,25,,,+C15
=,16,=,18,19,27,26
=,17,=,19,20,28,27
=,18,=,20,21,29,28
=,19,=,21,22,30,29
=,20,=,22,23,31,30
=,21,=,23,24,32,31,,,+C21
=,22,=,25,26,34,33,,,+C22
=,23,=,26,27,35,34
=,24,=,27,28,36,35
=,25,=,28,29,37,36
=,26,=,29,30,38,37
=,27,=,30,31,39,38
=,28,=,31,32,40,39,,,+C28
=,29,=,33,34,42,41,,,+C29
=,30,=,34,35,43,42
=,31,=,35,36,44,43
=,32,=,36,37,45,44
=,33,=,37,38,46,45
=,34,=,38,39,47,46
=,35,=,39,40,48,47,,,+C35
=,36,=,41,42,50,49,,,+C36
=,37,=,42,43,51,50
=,38,=,43,44,52,51
=,39,=,44,45,53,52
=,40,=,45,46,54,53
=,41,=,46,47,55,54
=,42,=,47,48,56,55,,,+C42
=,43,=,49,50,58,57,,,+C43
=,44,=,50,51,59,58
=,45,=,51,52,60,59
=,46,=,52,53,61,60
=,47,=,53,54,62,61
=,48,=,54,55,63,62
=,49,=,55,56,64,63,,,+C49
=,50,=,57,58,66,65,,,+C50
=,51,=,58,59,67,66
=,52,=,59,60,68,67
=,53,=,60,61,69,68
=,54,=,61,62,70,69
=,55,=,62,63,71,70
=,56,=,63,64,72,71,,,+C56
=,57,=,65,66,74,73,,,+C57
=,58,=,66,67,75,74
=,59,=,67,68,76,75
=,60,=,68,69,77,76
=,61,=,69,70,78,77
=,62,=,70,71,79,78
```

```
=,63,=,71,72,80,79,,,+C63
=,64,=,73,74,82,81,,,+C64
=,65,=,74,75,83,82
=,66,=,75,76,84,83
=,67,=,76,77,85,84
=,68,=,77,78,86,85
=,69,=,78,79,87,86
=,70,=,79,80,88,87,,,+C70
=,71,=,81,82,90,89,,,+C71
=,72,=,82,84,91,90
=,73,=,84,85,92,91
=,74,=,85,86,93,92
=,75,=,86,87,94,93
=,76,=,87,88,95,94,,,+C76
=,77,=,89,90,97,96,,,+C77
=,78,=,90,91,98,97
=,79,=,91,92,99,98
=,80,=,92,93,100,99
=,81,=,93,94,101,100
=,82,=,94,95,102,101,,,+C82
$ CONTINUATION CARDS (THICKNESS)
+C1,,,0.,,,0.
+C8,,,=,,,=
+C15,,,=,,,=
+C22,,,=,,,=
+C29,,,=,,,=
+C36,,,=,,,=
+C43,,,=,,,=
+C50,,,=,,,=
+C57,,,=,,,=
+C64,,,=,,,=
+C71,,,=,,,=
+C77,,,=,,,=
+C7,,,,0.,0.,
+C14,,,,=,=
+C21,,,,=,=
+C28,,,,=,=
+C35,,,,=,=
+C42,,,,=,=
+C49,,,,=,=
+C56,,,,=,=
+C63,,,,=,=
+C70,,,,=,=
+C76,,,,=,=
+C82,,,,=,=
$BALSA ELEMENTS AND CONT. CARDS
CQUAD4,102,50,2,3,11,10,,,+C102
=,103,50,3,4,12,11,,,+C103
=,104,50,4,5,13,12,,,+C104
=,105,=,5,6,14,13,,,+C105
=,106,=,6,7,15,14,,,+C106
=,109,=,10,11,19,18,,,+C109
=,110,=,11,12,20,19,,,+C110
=,111,=,12,13,21,20,,,+C111
```

```
=,112,=,13,14,22,21,,,+C112
=,113,=,14,15,23,22,,,+C113
=,116,=,18,19,27,26,,,+C116
=,117,=,19,20,28,27,,,+C117
=,118,=,20,21,29,28,,,+C118
=,119,=,21,22,30,29,,,+C119
=,120,=,22,23,31,30,,,+C120
=,123,=,26,27,35,34,,,+C123
=,124,=,27,28,36,35,,,+C124
=,125,=,28,29,37,36,,,+C125
=,126,=,29,30,38,37,,,+C126
=,127,=,30,31,39,38,,,+C127
=,130,=,34,35,43,42,,,+C130
=,131,=,35,36,44,43,,,+C131
=,132,=,36,37,45,44,,,+C132
=,133,=,37,38,46,45,,,+C133
=,134,=,38,39,47,46,,,+C134
=,137,=,42,43,51,50,,,+C137
=,138,=,43,44,52,51,,,+C138
=,139,=,44,45,53,52,,,+C139
=,140,=,45,46,54,53,,,+C140
=,141,=,46,47,55,54,,,+C141
=,144,=,50,51,59,58,,,+C144
=,145,=,51,52,60,59,,,+C145
=,146,=,52,53,61,60,,,+C146
=,147,=,53,54,62,61,,,+C147
=,148,=,54,55,63,62,,,+C148
=,151,=,58,59,67,66,,,+C151
=,152,=,59,60,68,67,,,+C152
=,153,=,60,61,69,68,,,+C153
=,154,=,61,62,70,69,,,+C154
=,155,=,62,63,71,70,,,+C155
=,158,=,66,67,75,74,,,+C158
=,159,=,67,68,76,75,,,+C159
=,160,=,68,69,77,76,,,+C160
=,161,=,69,70,78,77,,,+C161
=,162,=,70,71,79,78,,,+C162
=,165,=,74,75,83,82,,,+C165
=,166,=,75,76,84,83,,,+C166
=,167,=,76,77,85,84,,,+C167
=,168,=,77,78,86,85,,,+C168
=,169,=,78,79,87,86,,,+C169
=,172,=,82,84,91,90,,,+C172
=,173,=,84,85,92,91,,,+C173
=,174,=,85,86,93,92,,,+C174
=,175,=,86,87,94,93,,,+C175
=,178,=,90,91,98,97,,,+C178
=,179,=,91,92,99,98,,,+C179
=,180,=,92,93,100,99,,,+C180
=,181,=,93,94,101,100,,,+C181
+C102,,,.00,.66,.60,0.
+C103,,,.66,.97,.89,.60
+C104,,,.97,.97,.89,.89
+C105,,,.97,.66,.60,.89
+C106,,,.66,0.,0.,.60
```

```
+C109,,,0.,.60,.55,0.
+C110,,,.60,.89,.81,.55
+C111,,,.89,.89,.81,.81
+C112,,,.89,.60,.55,.81
+C113,,,.600,0.,0.,.550
+C116,,,.00,.55,.50,0.
+C117,,,.55,.81,.74,.50
+C118,,,.81,.81,.74,.74
+C119,,,.81,.55,.50,.74
+C120,,,.550,0.,0.,.500
+C123,,,.00,.500,.460,0.
+C124,,,.50,.74,.67,.46
+C125,,,.74,.74,.67,.67
+C126,,,.74,.50,.46,.67
+C127,,,.50,.0,.0,.46
+C130,,,.00,.46,.42,0.
+C131,,,.46,.67,.61,.42
+C132,,,.67,.67,.61,.61
+C133,,,.67,.46,.42,.61
+C134,,,.46,0.,0.,.42
+C137,,,0.,.42,.38,0.
+C138,,,.42,.61,.56,.38
+C139,,,.61,.61,.56,.56
+C140,,,.61,.42,.38,.56
+C141,,,.42,0.,0.,.38
+C144,,,.00,.38,.34,.00
+C145,,,.38,.56,.50,.34
+C146,,,.56,.56,.50,.50
+C147,,,.56,.38,.34,.50
+C148,,,.38,0.,0.,.34
+C151,,,0.,.34,.32,0.
+C152,,,.34,.50,.46,.32
+C153,,,.50,.50,.46,.46
+C154,,,.50,.34,.32,.46
+C155,,,.34,0.,0.,.32
+C158,,,0.,.32,.28,0.
+C159,,,.32,.46,.40,.28
+C160,,,.46,.46,.40,.40
+C161,,,.46,.32,.28,.40
+C162,,,.32,0.,0.,.28
+C165,,,0.,.28,.25,0.
+C166,,,.28,.40,.36,.25
+C167,,,.40,.40,.36,.36
+C168,,,.40,.28,.25,.36
+C169,,,.28,0.,0.,.25
+C172,,,0.,.36,.26,0.
+C173,,,.36,.36,.33,.26
+C174,,,.36,.25,.26,.33
+C175,,,.25,.0,0.,.26
+C178,,,0.,.26,.23,0.
+C179,,,.26,.33,.30,.23
+C180,,,.33,.26,.23,.30
+C181,,,.26,0.,0.,.23
$MAT PROP. ID
PSHELL,20,30,.188,30,,30,,0.
```

```
MAT1,30,1.05+7,,.3334,.000262
PSHELL,50,60,1.+7,60,,60,,0.
MAT1,60,1.85+5,,.05,2.15-5
EIGR,10,SINV,.1,80.0,,,,,+EIGR
+EIGR,MAX
PARAM,GRDPNT,1
ENDDATA
```

References

1. Douglas Aircraft Co., New Commercial Programs: *Study of High-Speed Civil Transports.* NASA CR-4235, 1989.

2. Robins, A. Warner; Dollyhigh, Samuel M.; Beissner, Fred L., Jr.; Geiselhart, Karl; Martin, Glenn L.; Shields, E. W.; Swanson, E. E.; Coen, Peter G.; and Morris, Shelby J., Jr.: *Concept Development of a Mach 3.0 High-Speed Civil Transport.* NASA TM-4058, 1988.

3. Boeing Commercial Airplane Co.: *Advanced Concept Studies for Supersonic Vehicles.* NASA CR-159028, 1979.

4. Van Dam, C. P.: Swept Wing-Tip Shapes for Low-Speed Airplanes. *SAE Trans.*, Section 6, vol. 94, 1985, pp. 6.355 6.364.

5. Van Dam, C. P.: Induced-Drag Characteristics of Crescent-Moon-Shaped Wings. *J. Aircr.*, vol. 24, no. 2, Feb. 1987, pp. 115 119.

6. Ashenberg, J.; and Weihs, D.: Minimum Induced Drag of Wings With Curved Planform. *J. Aircr.*, vol. 21, no. 1, Jan. 1984, pp. 89 91.

7. Vijgen, P. M. H. W.; Van Dam, C. P.; and Holmes, B. J.: Sheared Wing-Tip Aerodynamics: Wind-Tunnel and Computational Investigation. *J. Aircr.*, vol. 26, no. 3, Mar. 1989, pp. 207 213.

8. Zimmer, H. (Leo Kanner Assoc., transl.): *The Significance of Wing End Configuration in Airfoil Design for Civil Aviation Aircraft.* NASA TM-75711, 1979.

9. Naik, D. A.; and Ostowari, C.: An Experimental Study of the Aerodynamic Characteristics of Planar and Non-Planar Outboard Wing Planforms. AIAA-87-0588, Jan. 1987.

10. Keller, Donald F.; and Bullock, Ellen Parker: *Span Reduction Effects of Flutter Characteristics of Arrow-Wing Supersonic Transport Configurations.* NASA TP-3077, 1991.

11. Dansberry, Bryan E.; Rivera, Jose A., Jr.; and Farmer, Moses G.: *An Experimental Study of Tip Shape Effects on the Flutter of Aft-Swept, Flat-Plate Wings.* NASA TM-4180, 1990.

12. Doggett, Robert V., Jr.; and Soistmann, David L.: Some Low-Speed Flutter Characteristics of Simple Low-Aspect-Ratio Delta Wing Models. *A Collection of Technical Papers, Part 3 AIAA/ASME/ASCE/AHS/ASC 30th Structures, Structural Dynamics and Materials Conference*, Apr. 1989, pp. 1442 1450. (Available as AIAA-89-1325-CP.)

13. Reed, Wilmer H., III: *Aeroelasticity Matters: Some Reflections on Two Decades of Testing in the NASA Langley Transonic Dynamics Tunnel.* NASA TM-83210, 1981.

14. *MSC/NASTRAN User's Manual MCS/NASTRAN Version 65.* MSR-39, MacNeal-Schwendler Corp., Nov. 1985.

15. Desmarais, Robert N.; and Bennett, Robert M.: *User's Guide for a Modular Flutter Analysis Software System (FAST Version 1.0).* NASA TM-78720, 1978.

16. Harder, Robert L.; and Desmarais, Robert N.: Interpolation Using Surface Splines. *J. Aircr.*, vol. 9, no. 2, Feb. 1972, pp. 189 191.

17. Watkins, Charles E.; Woolston, Donald S.; and Cunningham, Herbert J.: *A Systematic Kernel Function Procedure for Determining Aerodynamic Forces on Oscillating or Steady Finite Wings at Subsonic Speeds.* NASA TR R-48, 1959.

18. Sandford, Maynard C.; Abel, Irving; and Gray, David L.: *Development and Demonstration of a Flutter-Suppression System Using Active Controls.* NASA TR R-450, 1975.

Table I. Measured and Analytical Properties of Models

R_{LE}, in.	Wing mass,[a] slugs	c.g., (x, y), in.		Mode 1		Mode 2		Mode 3		Mode 4		Mode 5	
		Measured	Analytical	f_m, Hz	f_a, Hz	f_m, Hz	f_a, Hz	f_m, Hz	f_a, Hz	f_m, Hz	f_a, Hz	f_m, Hz	f_a, Hz
∞	0.690	(33.1,11.3)	(32.7,11.1)	6.7	5.8	22.7	22.9	38.4	35.5	52.5	53.8	86.3	84.6
200	0.651	(30.8,11.1)	(30.7,11.1)	6.2	5.7	20.0	20.3	38.4	37.6	46.4	47.9	74.0	76.1
80	0.674	(28.0,11.3)	(27.7,11.1)	6.8	6.3	18.4	18.4	39.0	38.1	49.7	48.2	65.6	67.2

[a]Measured and analytical wing mass are the same.

Table II. Experimental Flutter Results

M	q, psf	f_f, Hz	V_f, fps	ρ, slugs/ft^3	μ	V_I	Re	m_o, slugs	f_2, Hz	f_f/f_2
No curvature ($R_{LE} = \infty$)										
0.668	219.7	14.8	751.4	0.000779	62.90	0.398	1.547×10^6	0.597	22.7	0.65
0.787	209.9	13.4	873.4	0.000550	89.09	0.389	1.297	0.597	22.7	0.59
0.891	192.5	12.4	973.8	0.000406	120.69	0.373	1.093	0.597	22.7	0.55
0.937	171.4	11.6	1005.0	0.000339	144.54	0.352	0.971	0.597	22.7	0.51
0.971	147.7	10.8	1040.8	0.000273	179.49	0.327	0.809	0.597	22.7	0.48
R_{LE} = 200 in.										
0.597	181.6	14.1	676.2	0.000795	57.74	0.431	1.405×10^6	0.558	19.7	0.72
0.683	179.8	13.8	768.6	0.000609	75.37	0.429	1.236	0.558	19.7	0.70
0.788	172.2	12.6	876.6	0.000448	102.46	0.420	1.056	0.558	19.7	0.64
0.862	162.9	12.1	949.6	0.000361	127.15	0.408	0.937	0.558	19.7	0.61
0.924	148.0	11.1	1007.4	0.000292	157.19	0.389	0.815	0.558	19.7	0.56
0.958	130.1	10.4	1032.7	0.000244	188.11	0.365	0.712	0.558	19.7	0.53
0.990	115.5	9.4	1065.1	0.000204	225.00	0.344	0.616	0.558	19.7	0.48
R_{LE} = 80 in.										
0.625	204.9	14.1	709.3	0.000815	58.40	0.482	1.507×10^6	0.581	18.4	0.77
0.747	204.7	13.2	839.3	0.000582	81.79	0.482	1.292	0.581	18.4	0.72
0.825	198.0	12.3	917.7	0.000470	101.28	0.473	1.160	0.581	18.4	0.67
0.902	187.8	11.8	991.5	0.000382	124.61	0.461	1.038	0.581	18.4	0.64
0.952	168.9	11.0	1039.0	0.000313	152.08	0.437	0.900	0.581	18.4	0.60
0.964	152.7	10.3	1049.1	0.000277	171.84	0.415	0.810	0.581	18.4	0.56

Table III. Analytical Flutter Results

M	q, psf	f_f, Hz	V_f, fps	ρ, slugs/ft^3	μ	V_I	Re	m_o, slugs	f_2, Hz	f_f/f_2
No curvature ($R_{LE} = \infty$)										
0.60	227.0	14.9	669.6	0.001010	48.51	0.404	1.794 $\times 10^6$	0.597	22.7	0.66
0.80	206.0	13.2	892.8	0.000518	94.59	0.386	1.223	0.597	22.7	0.58
0.90	181.0	12.0	1004.4	0.000358	136.87	0.361	0.954	0.597	22.7	0.53
0.95	161.0	11.3	1060.2	0.000286	171.33	0.341	0.804	0.597	22.7	0.50
$R_{LE} = 200$ in.										
0.60	181.7	13.4	669.6	0.000810	56.67	0.431	1.439 $\times 10^6$	0.558	19.7	0.68
0.80	168.8	12.0	892.8	0.000423	108.51	0.415	1.002	0.558	19.7	0.61
0.90	148.2	10.9	1004.4	0.000294	156.12	0.390	0.783	0.558	19.7	0.55
0.95	131.0	10.1	1060.2	0.000233	197.00	0.366	0.655	0.558	19.7	0.51
$R_{LE} = 80$ in.										
0.60	200.1	13.7	669.6	0.000893	53.30	0.476	1.586 $\times 10^6$	0.581	18.4	0.74
0.80	190.1	12.5	892.8	0.000477	99.79	0.464	1.130	0.581	18.4	0.68
0.90	173.2	11.5	1004.4	0.000343	138.78	0.442	0.914	0.581	18.4	0.63
0.95	160.6	11.1	1060.2	0.000286	166.43	0.426	0.804	0.581	18.4	0.60

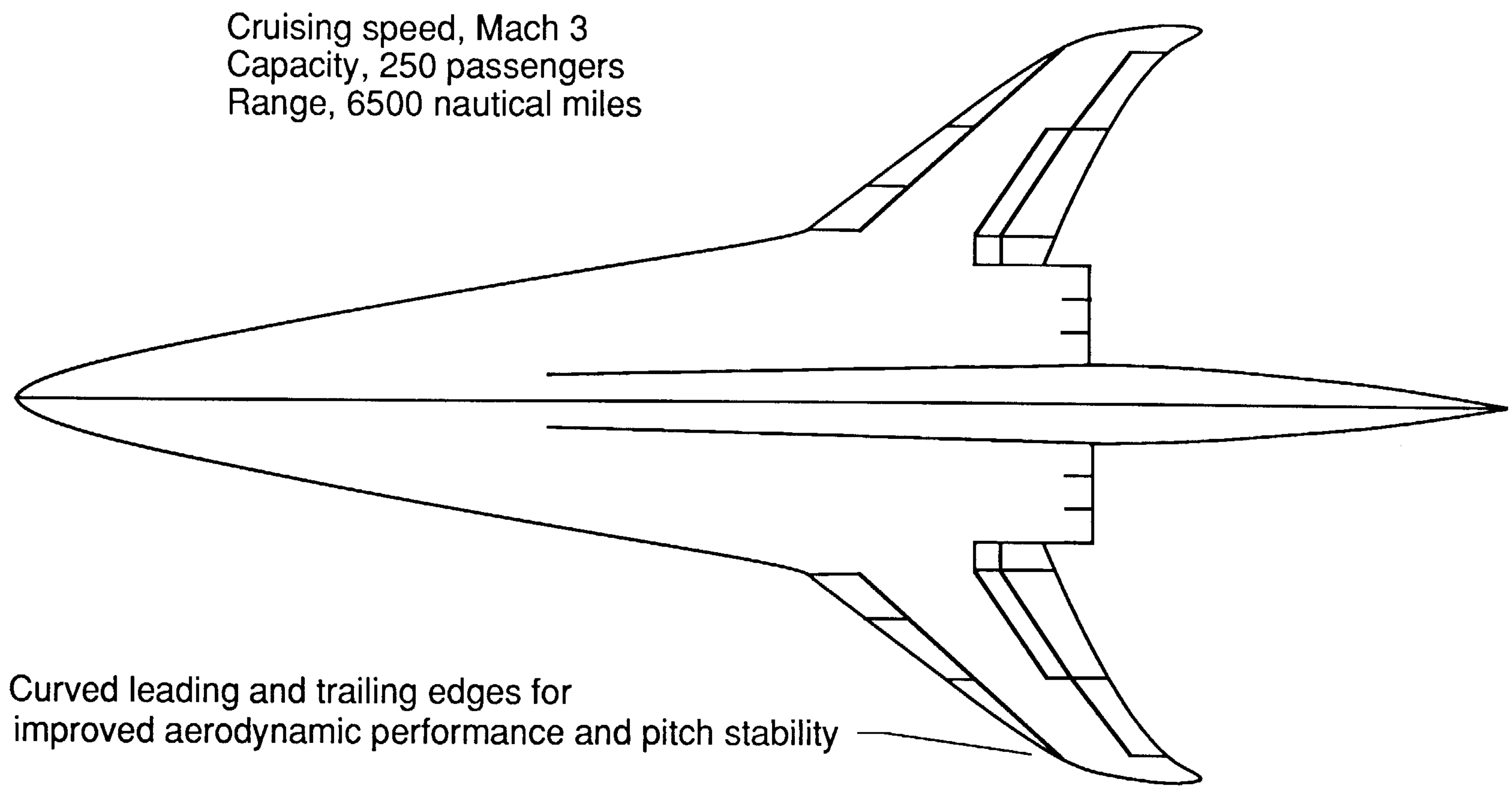

Figure 1. NASA High Speed Civil Transport concept.

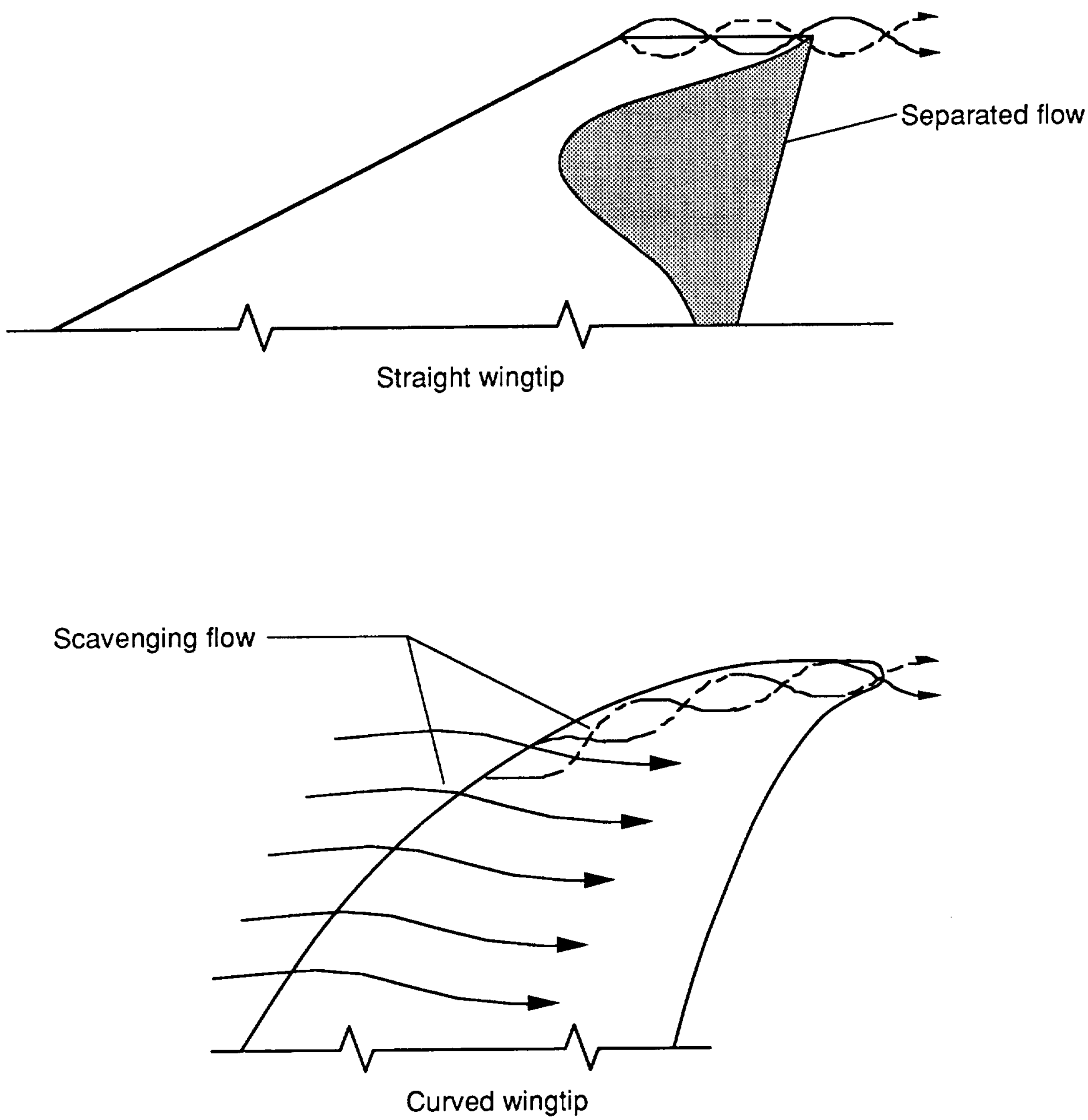

Figure 2. Wingtip flow for straight tip and curved tip.

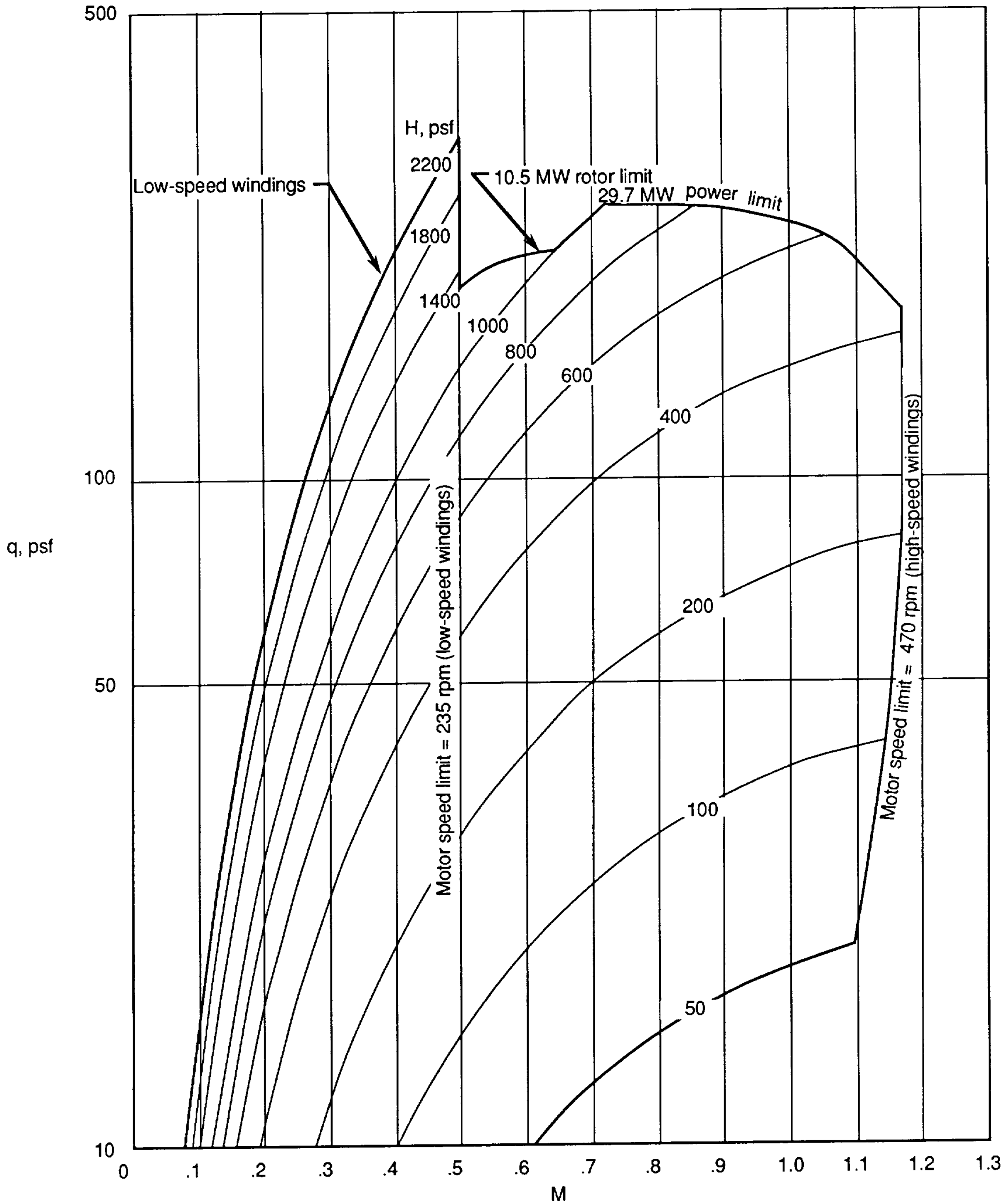

Figure 3. Transonic Dynamic Tunnel operating envelope for air.

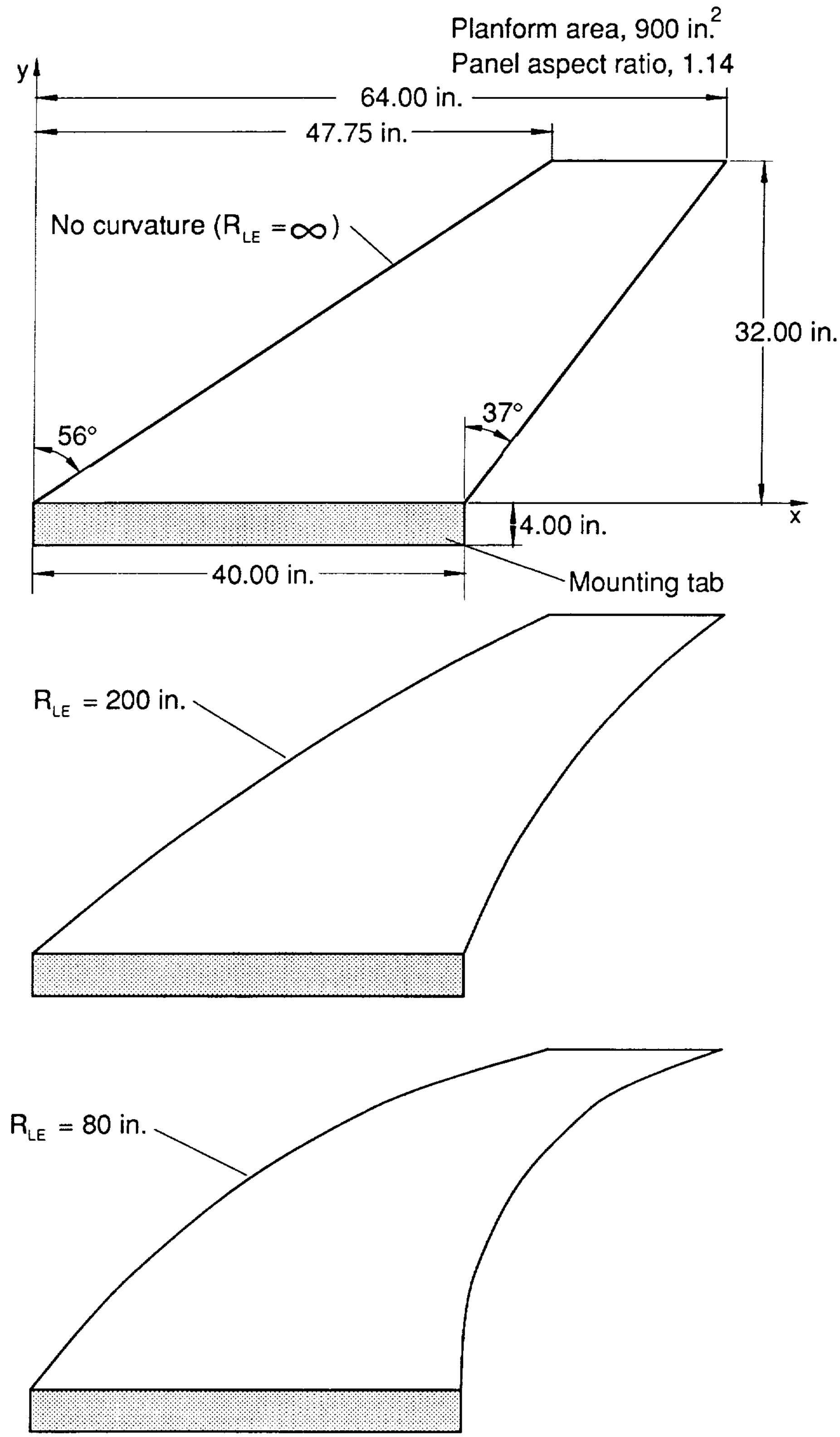

Figure 4. Model planforms.

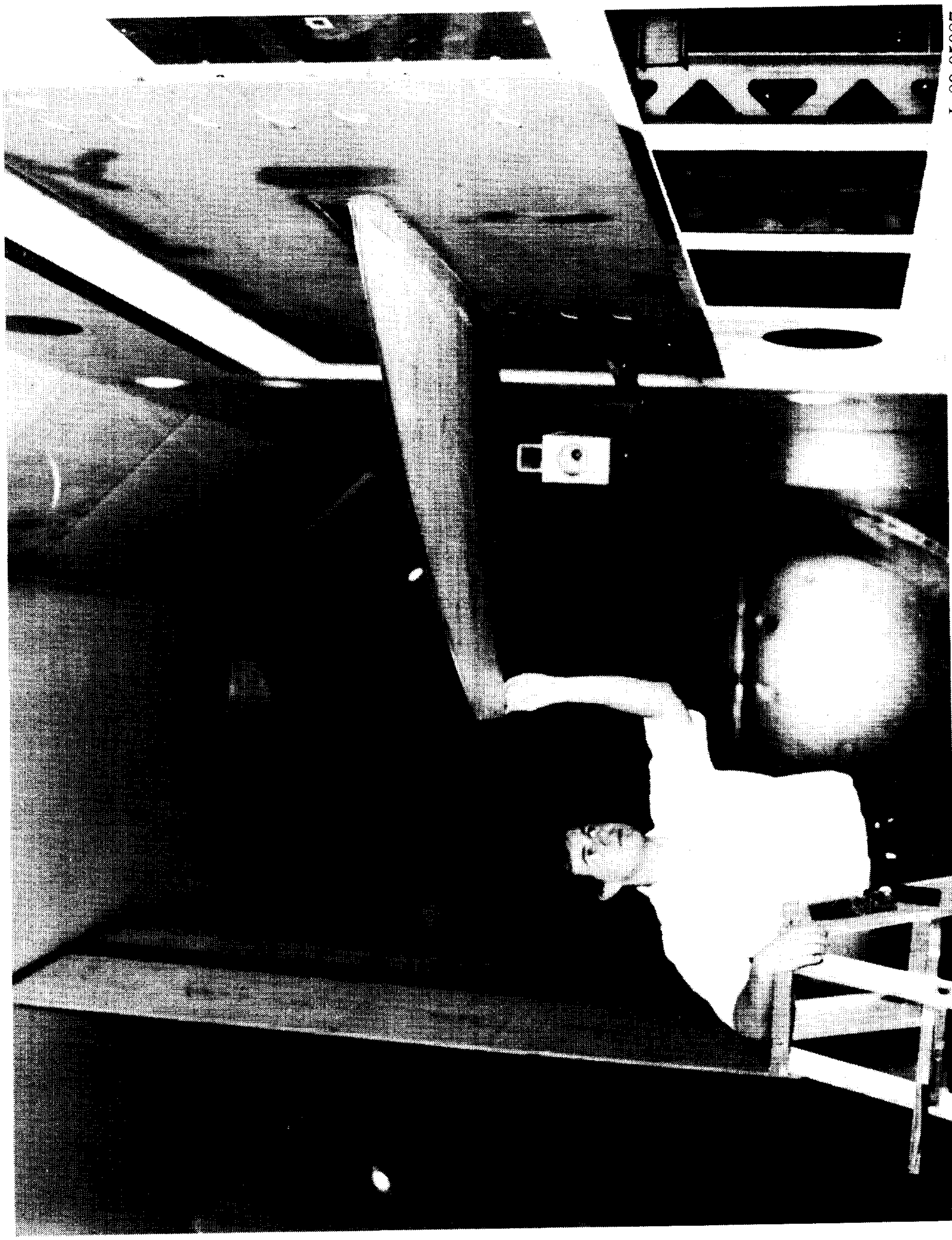

L-89-05087

Figure 5. Moderately curved model ($R_{LE} = 200$ in.) mounted in TDT.

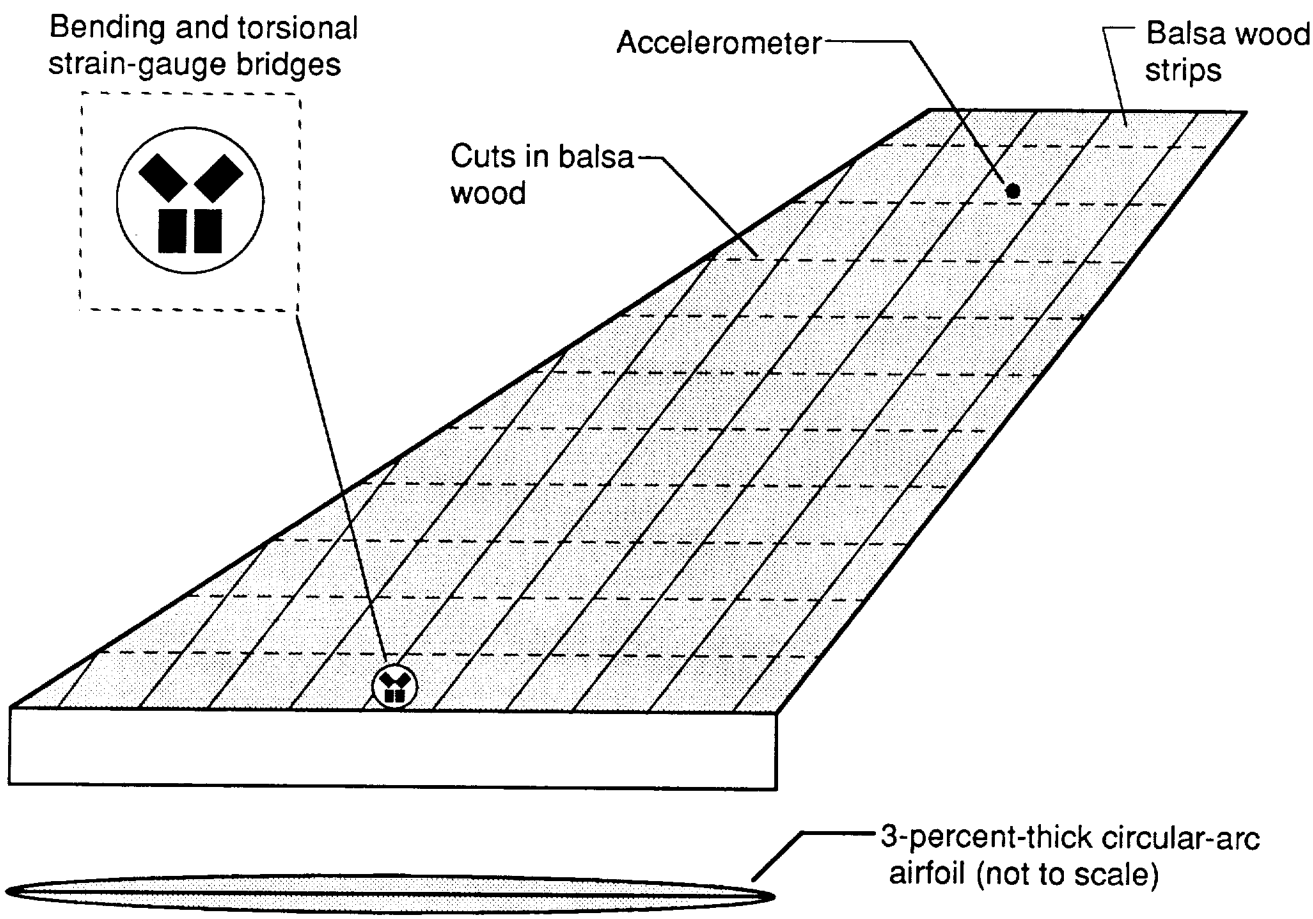

Figure 6. Model instrumentation and balsa wood layout (typical).

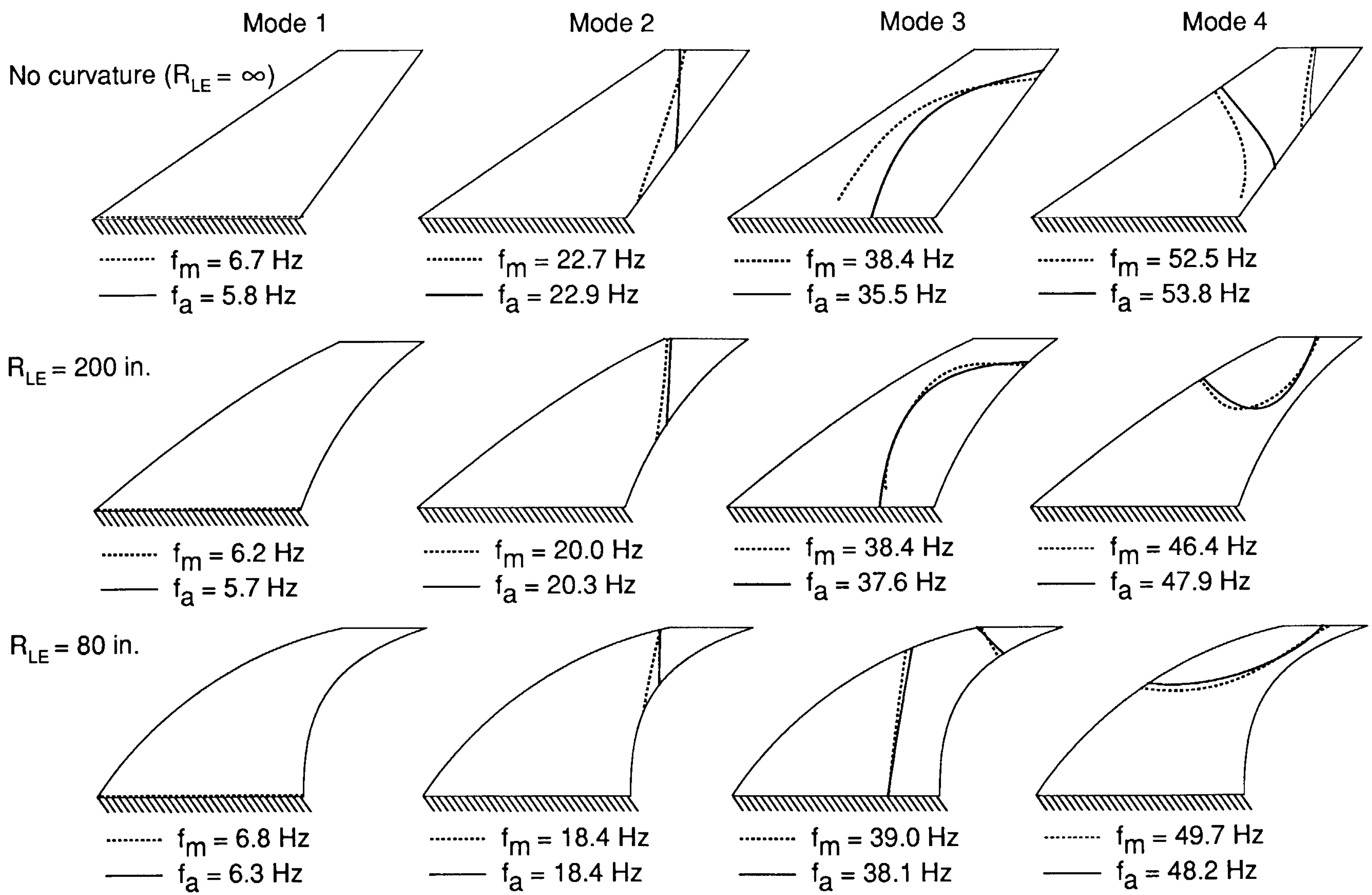

Figure 7. Experimental and analytical natural frequencies and node lines.

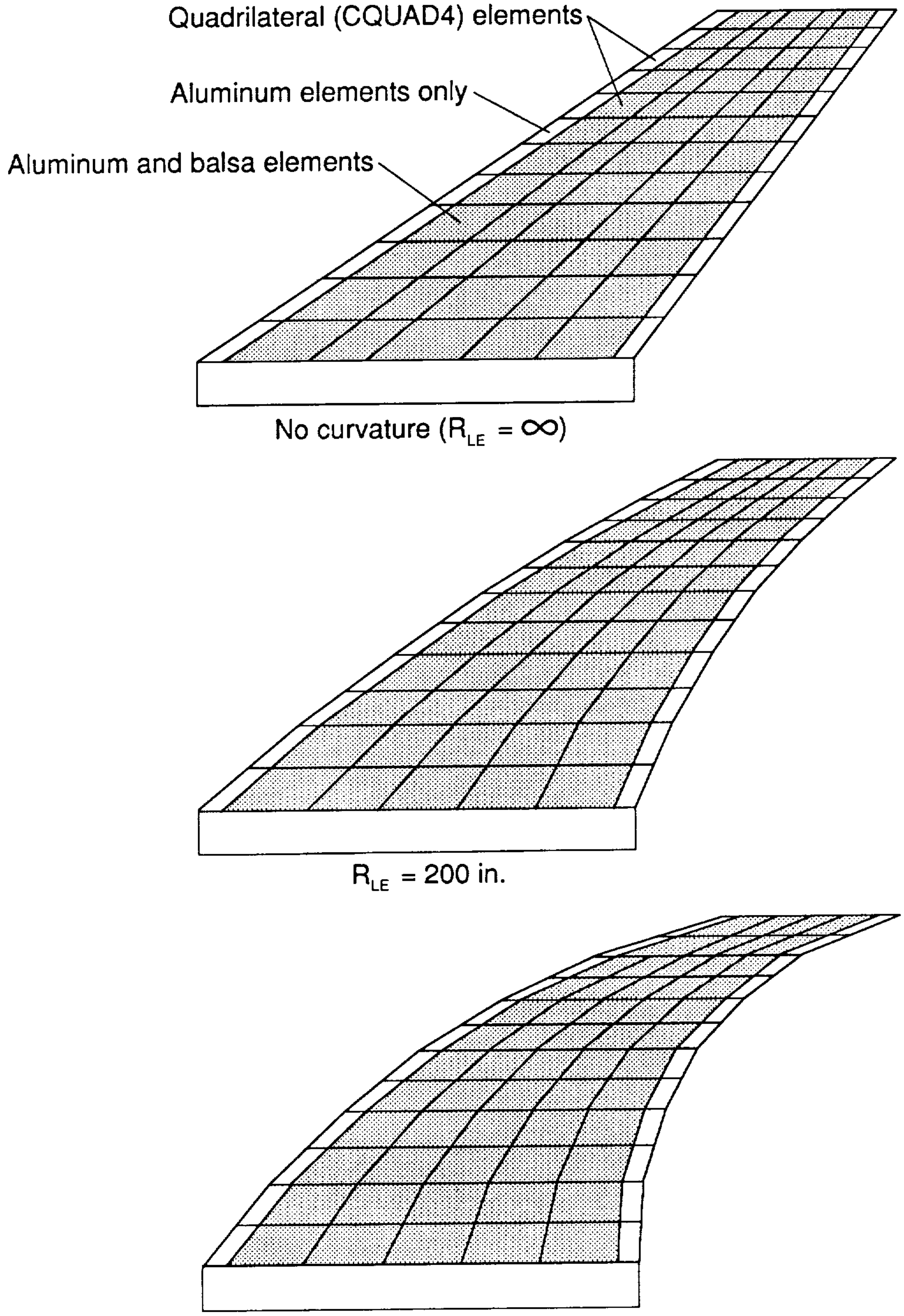

Figure 8. NASTRAN finite element models.

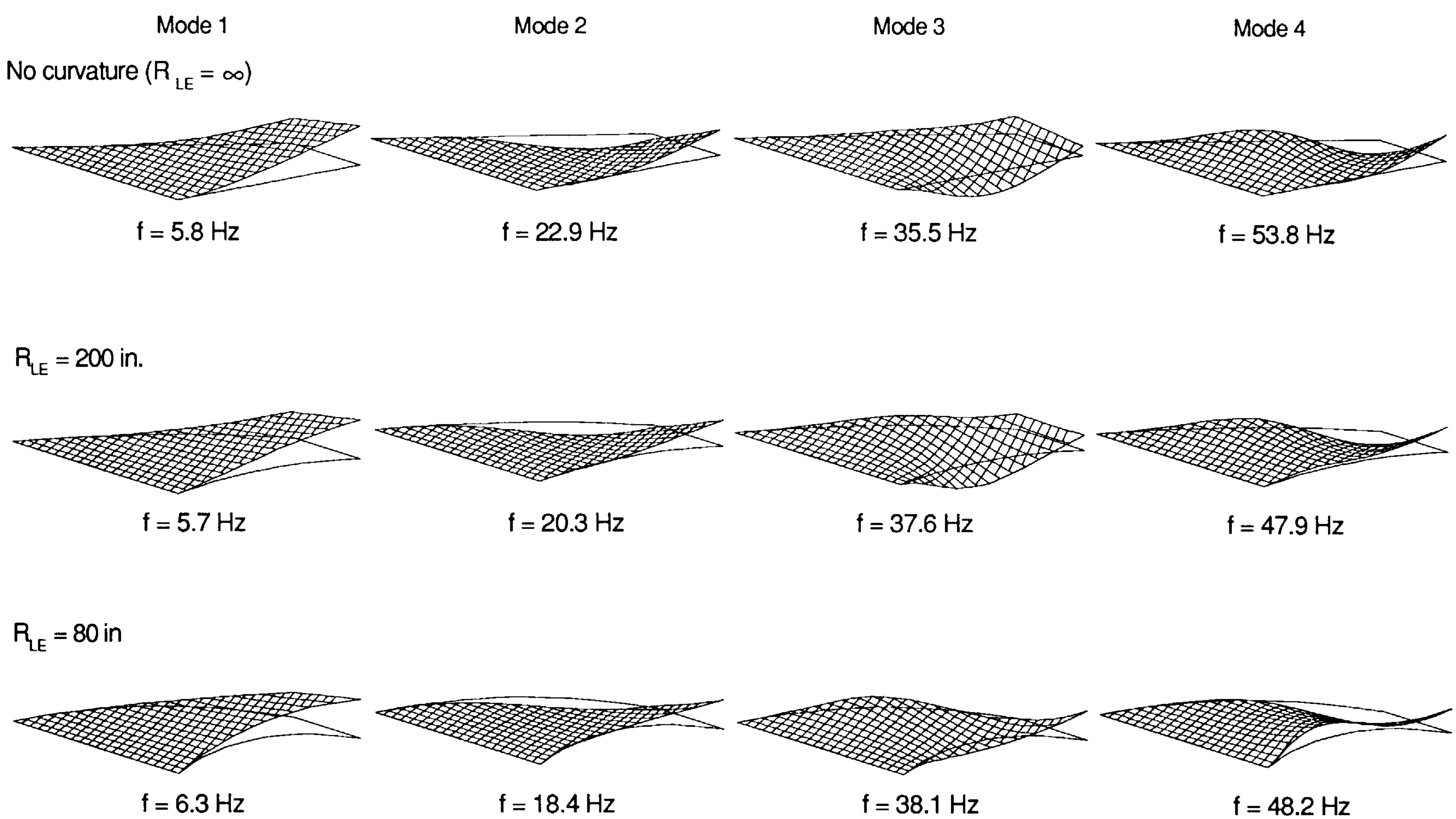

Figure 9. Analytical mode shapes and natural frequencies for first four natural vibration modes of the models.

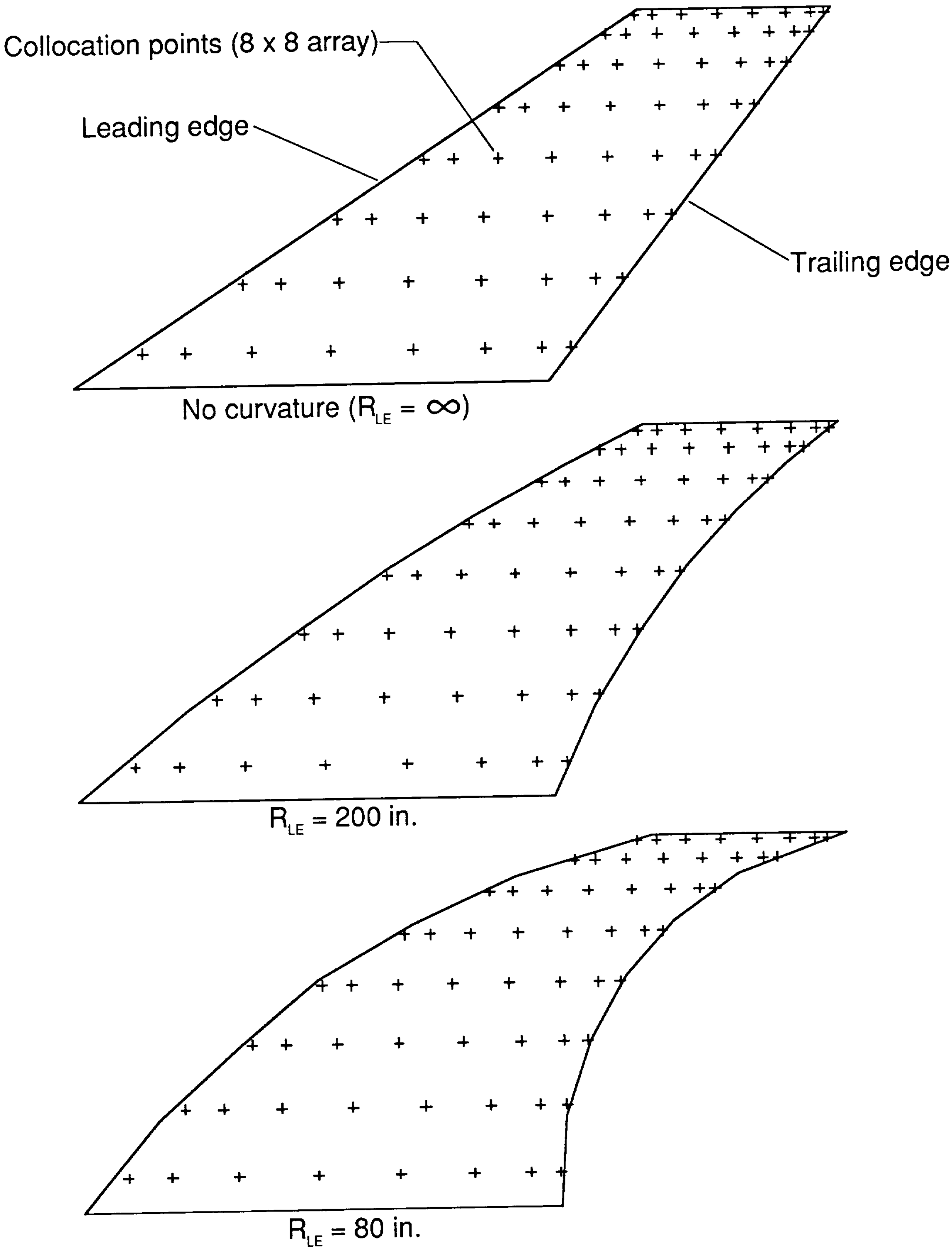

Figure 10. Collocation point locations (64) for subsonic kernel function analysis (FAST).

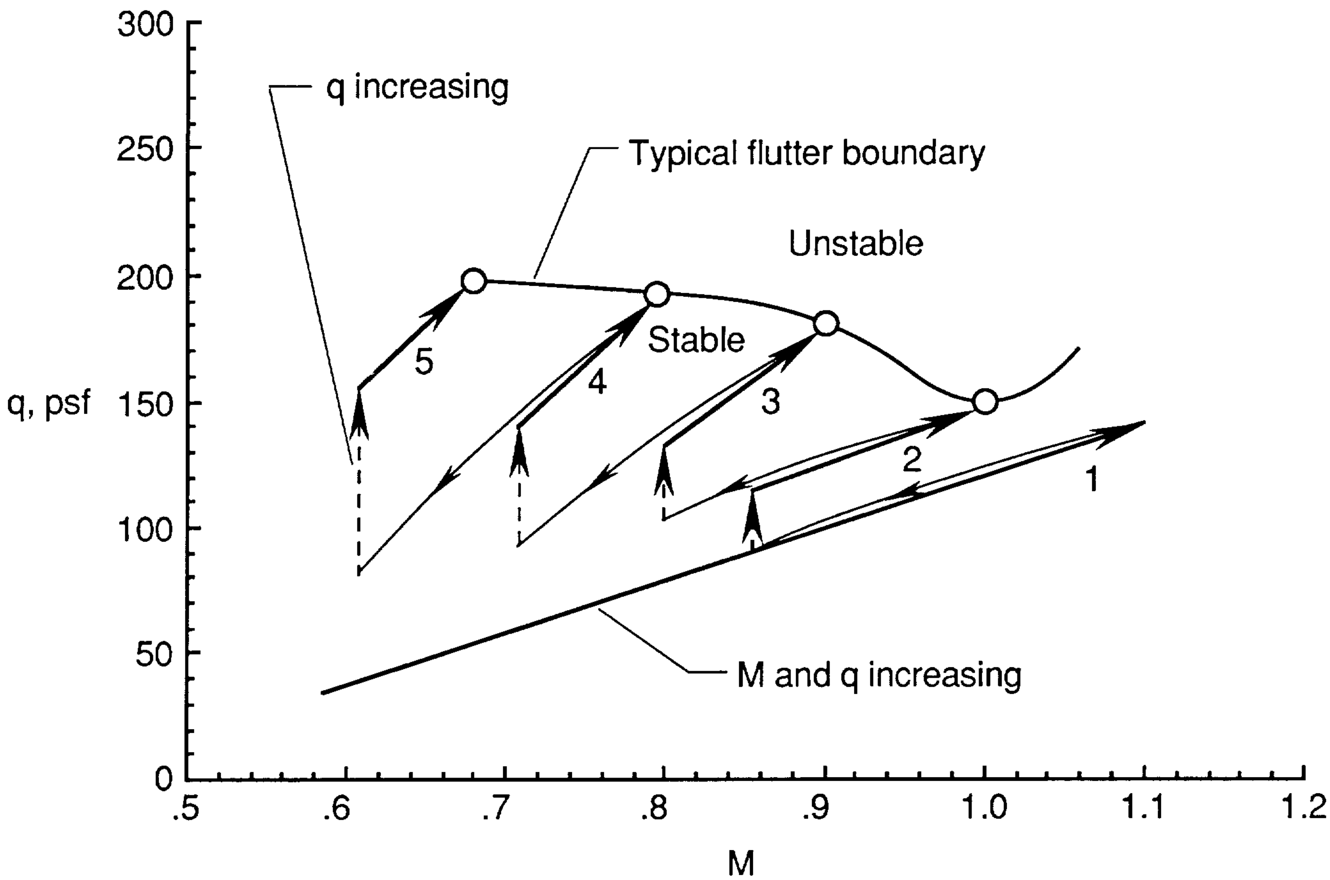

Figure 11. Wind-tunnel operating procedure.

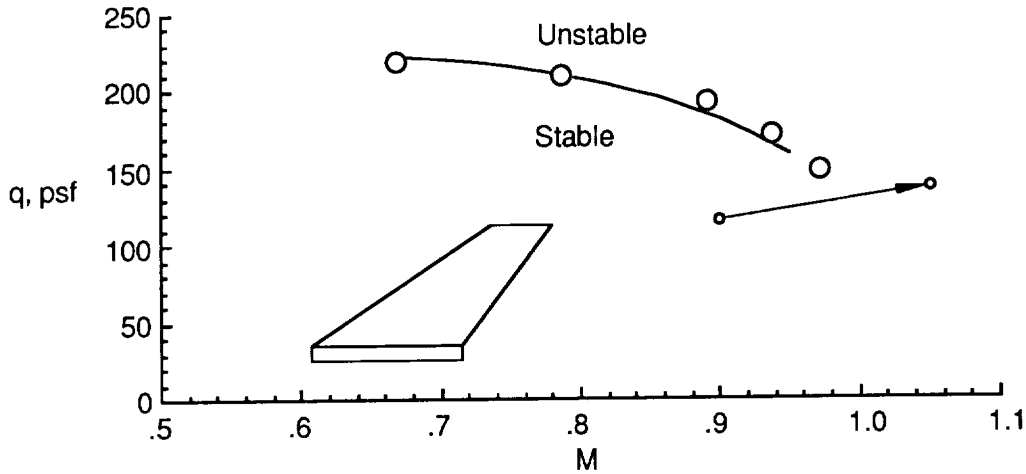

(a) Baseline model (no curvature).

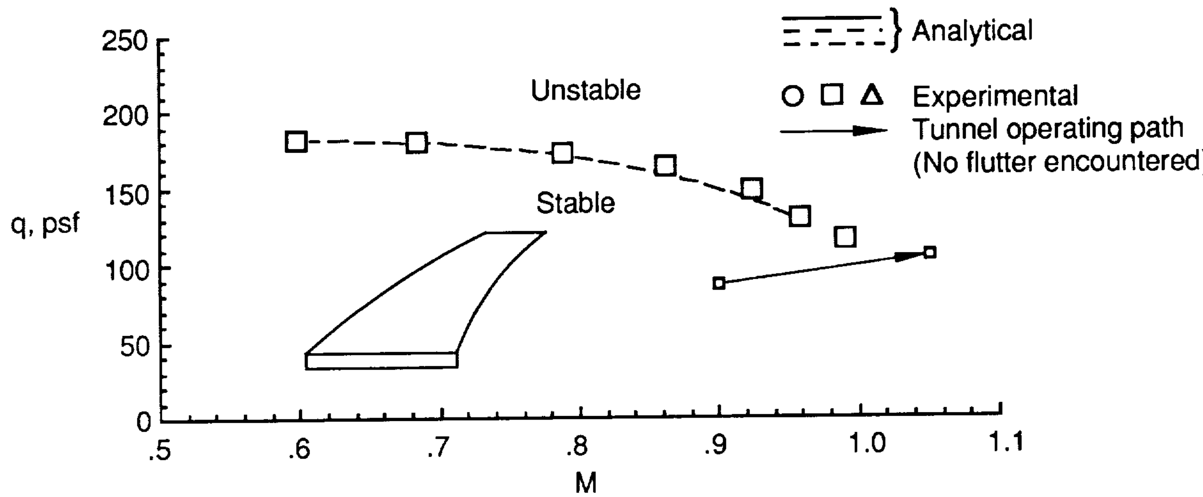

(b) $R_{LE} = 200$ in.

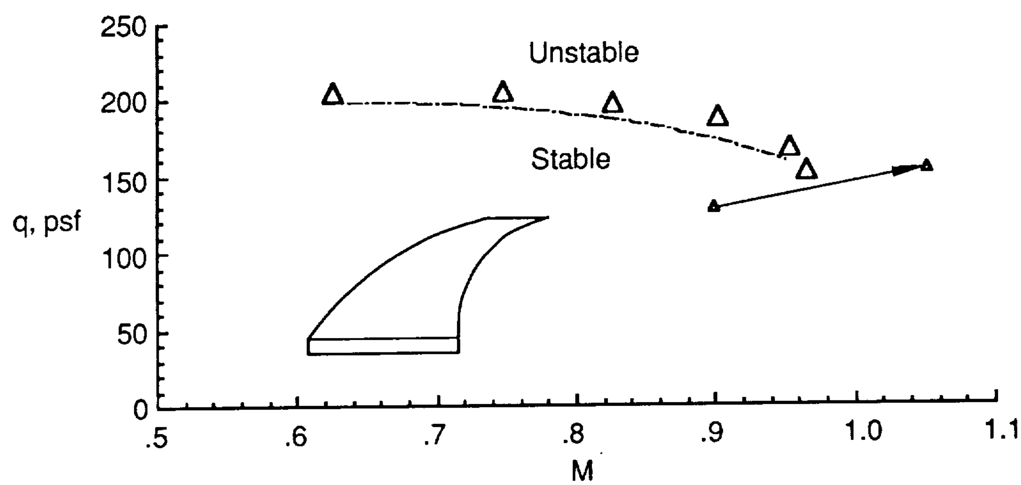

(c) $R_{LE} = 80$ in.

Figure 12. Experimental and analytical flutter dynamic pressure results.

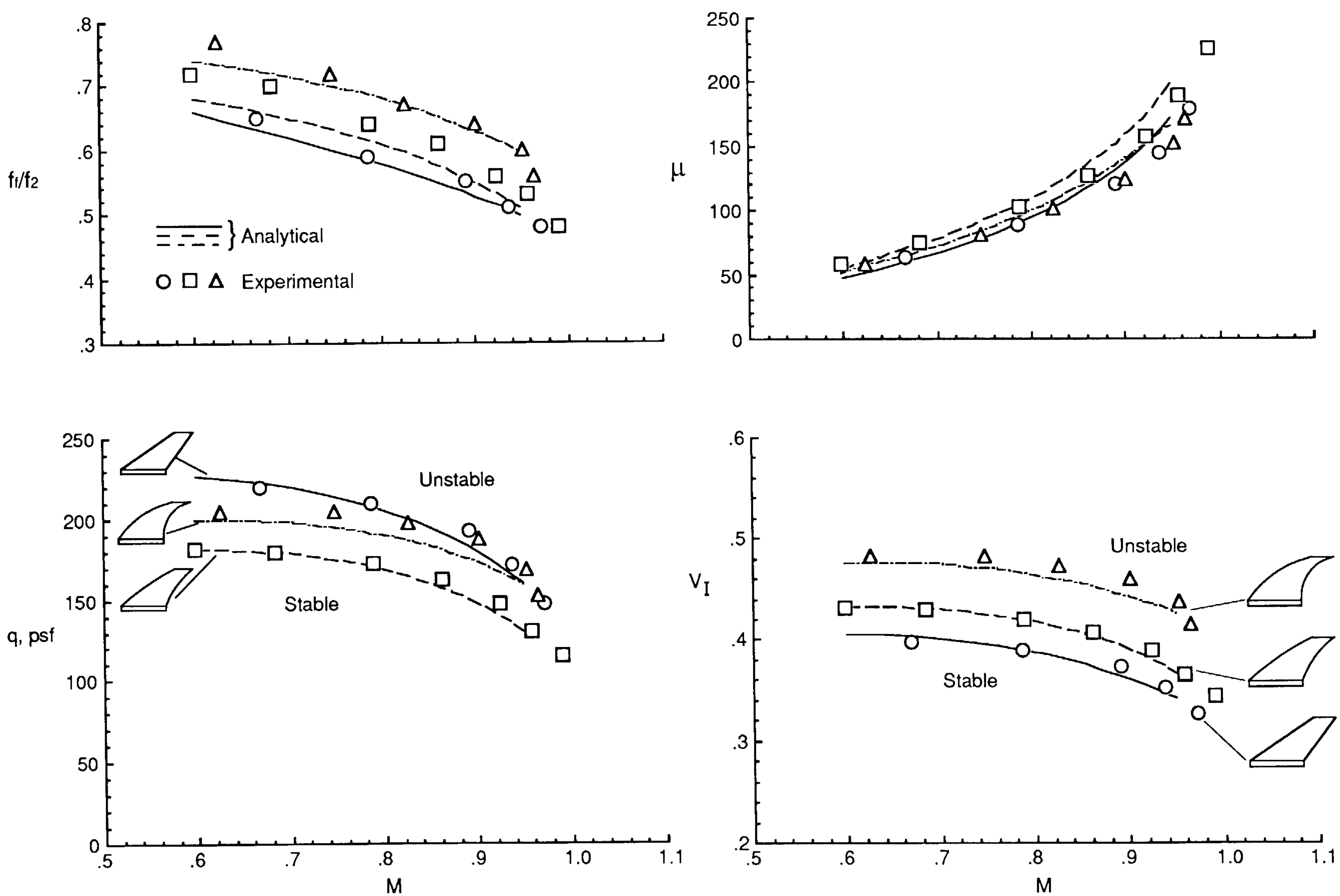

Figure 13. Experimental and analytical flutter results.

NASA
National Aeronautics and Space Administration

Report Documentation Page

1. Report No. NASA TP-3116	2. Government Accession No.	3. Recipient's Catalog No.
4. Title and Subtitle Planform Curvature Effects on Flutter Characteristics of a Wing With 56° Leading-Edge Sweep and Panel Aspect Ratio of 1.14		5. Report Date September 1991
		6. Performing Organization Code
7. Author(s) Donald F. Keller, Maynard C. Sandford, and Theresa L. Pinkerton		8. Performing Organization Report No. L-16858
9. Performing Organization Name and Address NASA Langley Research Center Hampton, VA 23665-5225		10. Work Unit No. 505-63-50-13
		11. Contract or Grant No.
12. Sponsoring Agency Name and Address National Aeronautics and Space Administration Washington, DC 20546-0001		13. Type of Report and Period Covered Technical Paper
		14. Sponsoring Agency Code

15. Supplementary Notes
Donald F. Keller and Maynard C. Sandford: Langley Research Center, Hampton, Virginia.
Theresa L. Pinkerton: University of Illinois, Urbana, Illinois.

16. Abstract
An experimental and analytical investigation was initiated to determine the effects of planform curvature (curving the leading and trailing edges of a wing in the X-Y plane) on the transonic flutter characteristics of a series of three moderately swept wing models. Experimental flutter results were obtained in the Langley Transonic Dynamics Tunnel for Mach numbers from 0.60 to 1.00, with air as the test medium. The models were semispan cantilevered wings with a 3-percent biconvex airfoil and a panel aspect ratio of 1.14. The baseline model had straight leading and trailing edges (i.e., no planform curvature). The radii of curvature of the leading edges of the other two models were 200 and 80 in. The radii of curvature of the trailing edges for these two models were determined so that the planform area of each of the three models was 900 in^2. Wingspan and the length and location of the root and tip chords were identical for all three models. Experimental results showed that flutter-speed index and flutter frequency ratio increased as planform curvature increased (radius of curvature of the leading edge was decreased) over the test range of Mach numbers. Analytical flutter results were calculated with a subsonic flutter-prediction program and agreed well with the experimental results.

17. Key Words (Suggested by Author(s)) Planform curvature; Aeroelasticity; Flutter; High speed civil transport; Low aspect ratio; Semispan model; Transonic	18. Distribution Statement Unclassified—Unlimited Subject Category 05

19. Security Classif. (of this report)	20. Security Classif. (of this page)	21. No. of Pages	22. Price
Unclassified	Unclassified	44	A03

National Aeronautics and
Space Administration
Code NTT-4

Washington, D.C.
20546-0001

Official Business
Penalty for Private Use, $300

BULK RATE
POSTAGE & FEES PAID
NASA
Permit No. G-27

NASA

POSTMASTER: If Undeliverable (Section 158 Postal Manual) Do Not Return